Journal of Sedimentary Research

Journal of Sedimentary Research, 2006, v. 76, 41–59
Reseach Article
DOI: 10.2110/jsr.2006.12

ANCIENT LACUSTRINE HYPERPYCNITES: A DEPOSITIONAL MODEL FROM A CASE STUDY IN THE RAYOSO FORMATION (CRETACEOUS) OF WEST-CENTRAL ARGENTINA

CARLOS ZAVALA,[1,2] JUAN JOSÉ PONCE,[2] MARIANO ARCURI,[2] DANIEL DRITTANTI,[1] HUGO FREIJE,[2] AND MARCOS ASENSIO[2]

[1]*Departamento de Geología, Universidad Nacional del Sur, San Juan 670, 8000 Bahía Blanca, Argentina*
[2]*Instituto Argentino de Oceanografía, Consejo Nacional de Investigaciones Científicas y Técnicas, Camino de La Carrindanga 7.5 km, 8000 Bahía Blanca, Argentina*
e-mail: czavala@criba.edu.ar

ABSTRACT: **Hyperpycnal flows originate when sediment-laden fluvial discharges enter standing, lower-density water. Because of their excess density, the flows plunge near the river mouth and continue to travel basinward as a quasi-steady and fully turbulent underflow. The related deposits are hyperpycnites, and constitute a particular type of turbidite with poorly known facies and facies tracts. Although hyperpycnal flows seem to be quite common in present times, their occurrence in fossil strata is poorly documented. This paper addresses the characteristics and depositional processes of shallow lacustrine sandy hyperpycnites, on the basis of the field analysis of well-exposed Lower Cretaceous strata (Rayoso Formation) in the Neuquén Basin of west-central Argentina. The Rayoso Formation is composed of clastic (and minor evaporitic) red beds up to 1200 m thick, deposited in a shallow perennial lake of variable salinity affected by long-lived hyperpycnal flows. Main clastic facies are composed of fine-grained sandstones with climbing ripples and plane beds. Other common sandstone facies include massive beds and low-angle cross stratification. Most sandstone facies are related to traction plus fallout processes, and often show a vertical fluctuation between sedimentary facies originated under different traction-plus-fallout conditions within single beds. These fluctuations are interpreted to be evidence of deposition from flow fluctuations in sustained hyperpycnal flows. Most beds internally show the existence of three depositional phases, *acceleration (AP), erosion plus bypass (EP)*, and *deceleration (DP)*, which record the complete evolution of a single long-lived hyperpycnal flow at a fixed point. Additionally, the depositional evolution of a single long-lived hyperpycnal flow with distance records initially the progressive basinward migration of the AP and EP phases, and finally an overall deposition under the DP phase both in proximal and distal areas. This evolution provides an adequate explanation for the basinward extension of channelized features, and for the occurrence of fine-grained sandstones with climbing ripples both in proximal and distal positions within the same hyperpycnal system. Consequently, facies analysis derived from application of the Bouma sequence is not valid for deposits of quasi-steady hyperpycnal flows.**

INTRODUCTION

First recognized by Forel (1892) in Lake Geneva, sedimentation related to hyperpycnal flows in lacustrine and shallow marine environments has recently received increasing attention (Mulder and Syvitski 1995; Mutti et al. 1996; Mulder et al. 1998; Mutti et al. 2000; Mulder and Alexander 2001a, 2001 b; Alexander and Mulder 2002; Mellere et al. 2002; Mulder et al. 2003; Gani 2004; Plink-Björklund and Steel 2004). Hyperpycnal flows are formed when a sediment-laden fluvial discharge enters a standing body of water, mainly during a flood (Mulder and Syvitski 1995). If the excess density provided by the suspended load results in a flow with a bulk density greater than that of the reservoir, the flow will plunge (Bates 1953; Mutti et al. 1996) generating a subaqueous extension of the fluvial channel, and basinward delivery of a huge volume of sediment. Although direct fluvial discharge has been proposed as a valid triggering mechanism for surging (episodic) turbidity flows (Normark and Piper 1991; Mutti et al. 1996; Mutti et al. 1999; Stow and Mayall 2000), hyperpycnal flows are often characterized by long-lived and sustained discharges, with facies and facies associations which depart significantly from classical models (Alexander and Mulder 2002). Even if hyperpycnal flows seem to be quite common at the mouths of most contemporaneous rivers (cf. Forel 1892; Mulder and Syvitski 1995; Kineke et al. 2000; Johnson et al. 2001; Mulder et al. 2001), their occurrence in ancient deposits has been poorly documented in literature (Alexander and Mulder 2002; Mellere et al. 2002; Mutti et al. 2003; Plink-Björklund and Steel 2004).

Hyperpycnal flows are fully turbulent flows, and their deposits are a special kind of turbidite called hyperpycnites (Mulder et al. 2003). In the present paper the term "turbidity bed" refers to a specific depositional process, not always related to deep-marine turbidite systems.

A hyperpycnal system could be defined as the subaqueous extension of the fluvial system originated by hyperpycnal fluvial discharges. Consequently, their deposits and depositional features could resemble some common characteristics of both fluvial and turbidite deposits.

Because the generation of a hyperpycnal flow is related to the density contrast between the incoming flow and the receiving water body, lacustrine systems seem to be the most susceptible to receive periodic fluvial-derived underflows because of the relative lower density of fresh water bodies (Bates 1953; Mulder and Alexander 2001a; Alexander and Mulder 2002). For most geologists, the existence of deposits displaying channelized clastic bodies (often filled with sandstone and conglomerate)

 1527-1404/06/076-041/$03.00

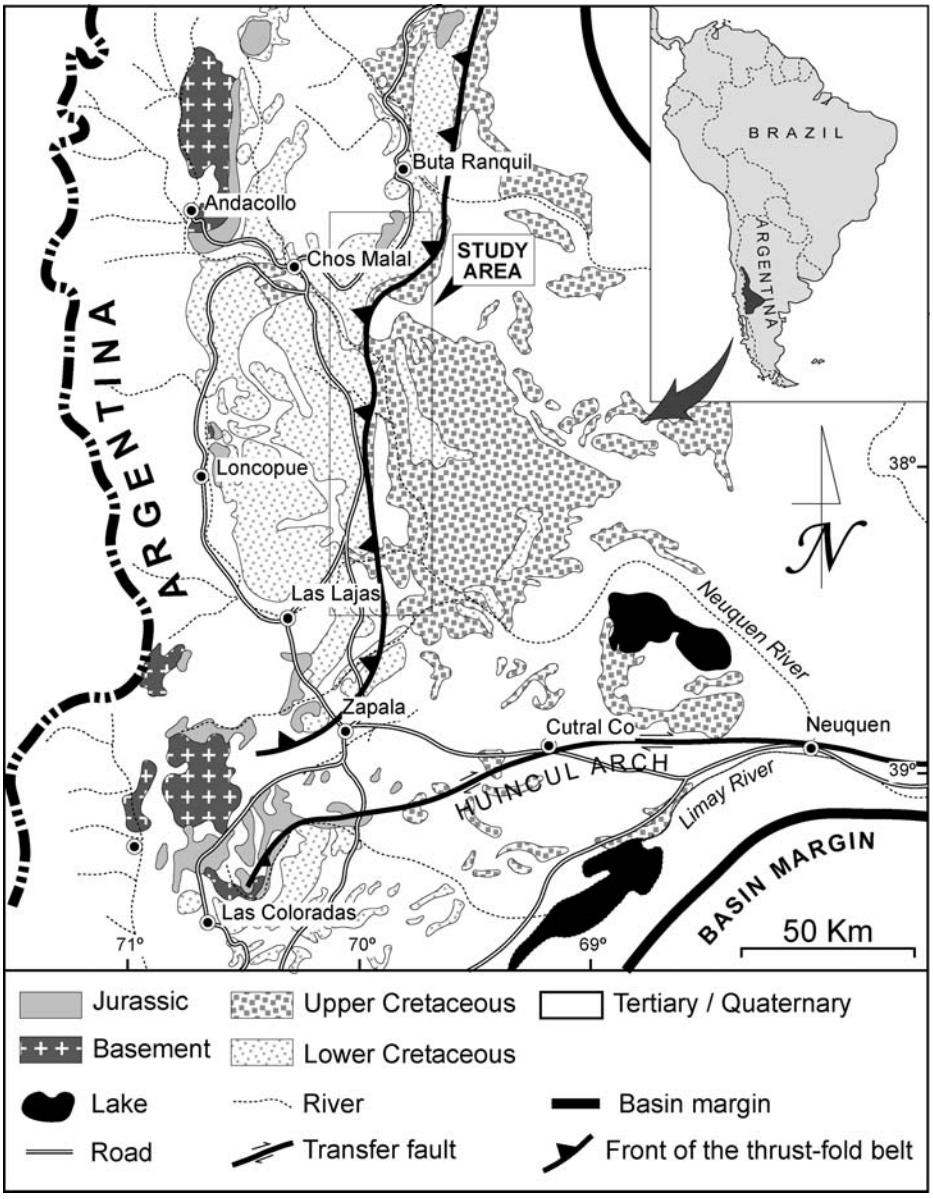

FIG. 1.—Simplified geologic map of the Neuquén Basin in west-central Argentina. The studied area is located close to the buried frontal thrust belt, where the best exposures of the Rayoso Formation are located. Modified after Gulisano and Gutierrez Pleimling (1995).

associated with reddish mudstone suggests a subaerial fluvial origin. Controversially, although both experimental studies and observations from modern environments (Dott 1963; Giovanoli 1990; Twichell et al. 2005) support the common occurrence of channels in subaqueous lacustrine systems, the related deposits have been poorly documented in literature for ancient successions. It is possible that many ancient hyperpycnites have been misinterpreted in the past as fluvial deposits (Mutti et al. 1996; Mutti et al. 2000), thus requiring further studies.

This paper focuses on the analysis and discussion of sedimentary structures, facies, and depositional features which are typical of hyperpycnal deposits, with special reference to the Cretaceous Rayoso Formation that crops out in west-central Argentina (Neuquén Basin). The Rayoso Formation is composed of a mainly clastic succession up to 1200 m thick with an areal distribution that exceeds 6×10^4 km^2. These strata are characterized mainly by fine- to medium-grained sandstones, mudstones, and minor carbonates and evaporites deposited in a shallow perennial lake. To the best of our knowledge, this paper describes for the first time ancient lacustrine hyperpycnites from an outcrop perspective.

In recent years, the increasing petroleum production from clastic bodies of the Rayoso Formation provided new frontiers for hydrocarbon exploration and development in the Neuquén Basin, because of the relatively shallow occurrence of the reservoirs and overall good petrophysical properties. Nevertheless, commercial production from these strata requires the application of sophisticated production strategies, which necessitate a comprehensive and precise understanding of the three-dimensional characteristics of clastic bodies. This has recently encouraged new efforts to develop geological models of the unit (Zavala et al. 2001; Ponce et al. 2002), accompanied by a general revision of its stratigraphy. The recent advances in the understanding of depositional processes of clastic units affected by relatively long-lived hyperpycnal flows provide new tools for the stratigraphic analysis and understanding of facies changes and internal geometry of related depositional bodies.

GEOLOGICAL SETTING

Located in the Southern Andes, the Neuquén Basin is the main oil-bearing basin of Argentina (Fig. 1). The Neuquén basin is a triangular-

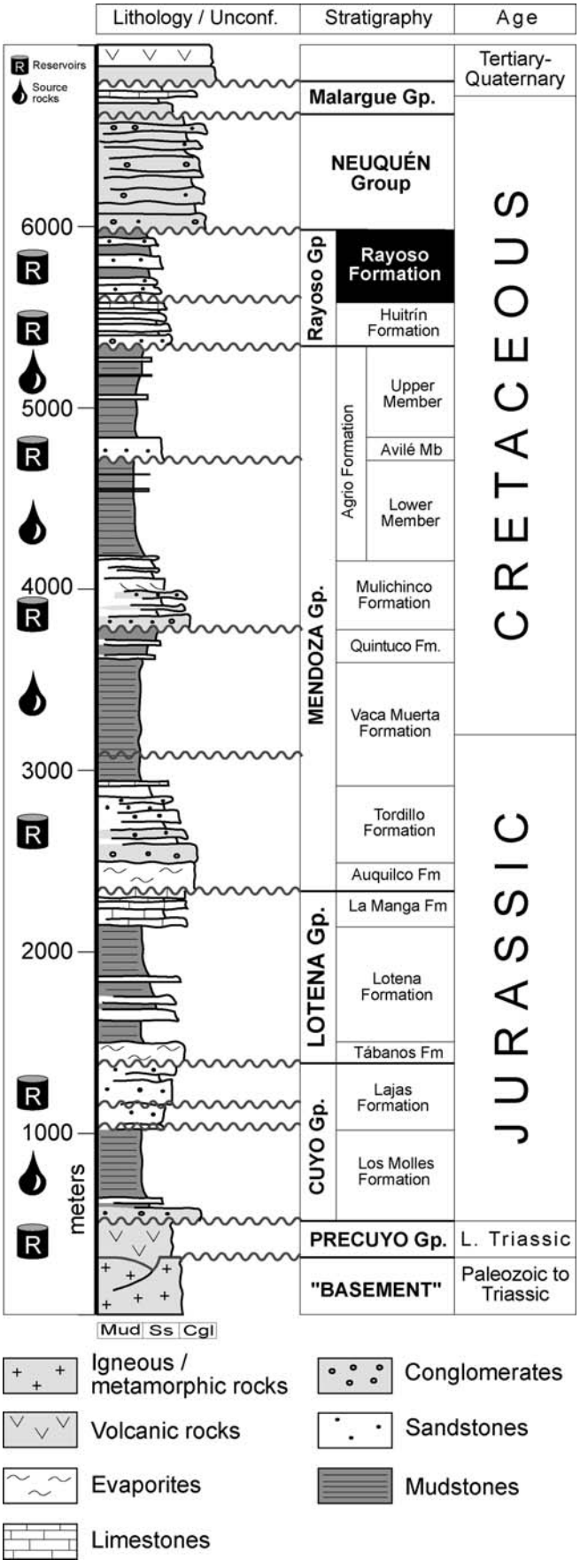

shaped basin covering more than 160,000 km^2, and it corresponds to the southern end of a series of marine sedimentary basins developed close to the western margin of Gondwana during the Mesozoic (Fig. 1). The origin of the Neuquén Basin is related to the convergence of the South American lithospheric plate with the southern segment of the Nazca–Pacific Plate (Hogg 1993). This basin has been interpreted as a back-arc basin, with an origin related to the thermal-tectonic collapse of the continental crust behind a stationary magmatic arc during the Late Triassic (Mpodozis and Ramos 1989: Vergani et al. 1995). The basin fill records at least 220 Ma of basin subsidence, and consists of an Upper Triassic–Cenozoic siliciclastic (and minor carbonatic) succession that is at least 7000 m thick (Fig. 2). Deposits are mostly shallow marine in origin, and related to a prolonged connection with the Paleo-pacific Ocean. Nevertheless, the marine influence was interrupted several times by short periods according to sea-level variations (Mutti et al. 1994). These periods of marine disconnection are usually characterized by regional unconformities that display in places some angularity evidencing also a tectonic overprint. Accommodation space increased progressively above the basal unconformity, resulting in the accumulation of a transgressive succession consisting of continental and marine deposits. During the accumulation of this succession, three main depositional stages can be recognized (Zavala and González 2001): The first stage (Late Triassic–Early Jurassic) is syn-rift, characterized by deposition of volcanic and volcaniclastic materials (Precuyo Group) along with half-graben depocenters (Gulisano 1981). The second stage (Early–Late Jurassic) is represented by a mainly clastic prograding marine to continental succession (Cuyo and Lotena groups), deposited over a tectonically induced irregular relief. The third stage (Late Jurassic–Late Cretaceous) is a marine to continental succession up to 6 km thick (Mendoza, Rayoso, and Neuquén groups). These deposits have the most extensive geographical occurrence in the basin, and their thickness changes regularly. Additional information on the Neuquén Basin can be found in Hogg (1993) and Vergani et al. (1995).

The marine influence from the Pacific Ocean started in the Early Jurassic, and extended more or less continuously until the late Early Cretaceous, when the basin was definitively disconnected. As a consequence, a thick succession of continental deposits accumulated, starting with fine-grained red beds of the Rayoso Formation (Groeber 1946, 1953; Herrero Ducloux 1946). This unit is composed of a succession, up to 1200 m thick, of fine sandstones, red mudstones, and minor evaporites, distributed over 6×10^4 km^2 (Zollner and Amos 1973; Uliana et al. 1975a, 1975b; Legarreta 1985; Ramos 1981).

The Rayoso Formation sharply overlies the calcareous strata of the Huitrín Formation, and it is unconformably covered by coarse-grained continental red beds of the Neuquén Group (Fig. 2). Earlier works suggested for the unit an origin related to ephemeral fluvial systems with large associated floodplains (Uliana et al. 1975b), while others (Legarreta 1985) recognized high-sinuosity channels within tidally influenced mudflats. More recently Zavala et al. (2001) and Ponce et al. (2002) discussed the stratigraphy and depositional model of the Rayoso Formation, and concluded that the unit most likely accumulated in a shallow perennial lake of variable salinity affected by long-lived hyperpycnal flows. Recent studies on paleontology and biostratigraphy strongly support a lacustrine origin of the Rayoso Formation. The succession displays an association of charophytes, nonmarine ostracods, small dinoflagellates, and hypohaline foraminifers, which are indicative of a lacustrine environment (Musacchio and Vallati 2000). In addition, the widespread occurrence of stromatolites suggests shallow-water conditions, with almost the entire water body being in the photic zone.

←

FIG. 2.—Schematic stratigraphic column of the Neuquén Basin with indication of the main hydrocarbon source and reservoir rocks. The stratigraphic position of the Lower Cretaceous Rayoso Formation is indicated.

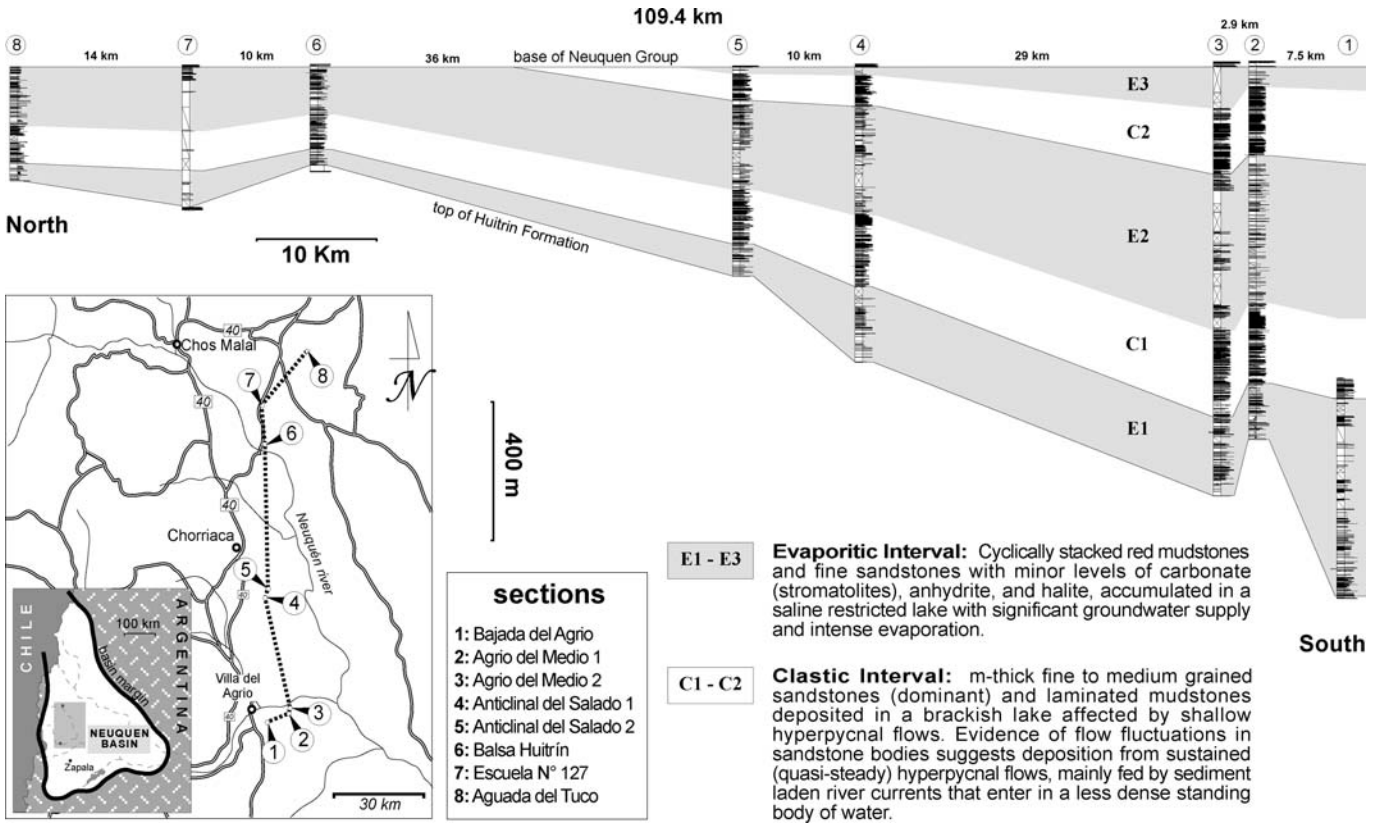

FIG. 3.—Regional cross section of the Rayoso Formation across 109.4 km, referenced to the base of the Neuquén Group. Three evaporitic and two clastic intervals can be observed. Note also the large scale truncation of upper intervals towards the north.

FACIES ANALYSIS AND DEPOSITIONAL MODEL

The existence of excellent and laterally continuous exposures of the Rayoso Formation allowed a detailed and extensive field investigation aimed at the understanding of facies and stratigraphy. Nine detailed stratigraphic sections of the whole succession were measured and correlated (Fig. 3) using conventional and photostratigraphic tools. A complete simplified section of the unit is shown in Figure 4A. Detailed description of field exposures permitted the discrimination of 14 clastic and evaporitic facies (outlined in Table 1). Clastic facies are dominantly fine-grained (mostly finer than medium sandstone), with little variation through the whole studied area. No coeval coarse-grained sandstone or conglomerate facies have been identified. The main clastic facies is fine-grained sandstone with climbing ripples (facies Scr, Figs. 5E, 6B, C), which is widely distributed as tabular and channelized bodies. Other common facies include laminated (facies Sl, 5D, E, 6C) and massive sandstone beds (facies Sm, Figs. 5A, D). Laminated sandstones are common in tabular and irregular bodies, while massive sandstones are more frequent filling erosional depressions. Strata with low angle cross-stratification (facies Scs, Fig. 5A, B) are common in channel fills often displaying abundant mud clasts at the lower lee side. Isotropic hummocky cross-stratification (HCS) facies (facies Shi, Fig. 5C) have a minor significance and generally appear in tabular bodies.

Climbing ripples are depositional structures commonly developed in subaqueous environments, and they are related to traction-plus-fallout processes (Jopling and Walker 1968) generated by a turbulent flow with high suspended load (Mulder and Alexander 2001a). Recently, this structure has been considered as a major sedimentary feature in hyperpycnal turbidites, because it represents the steady migration of sedimentary bedforms while sediment supply is maintained and sedimentation rate is significant (Mulder and Alexander 2001a; Mulder et al. 2003). As noted by Sanders (1965), climbing ripples often pass laterally into laminated sandstones. Theoretical and experimental studies support the existence of plane-bed conditions also related to traction-plus-fallout processes (Banerjee 1977; Arnott and Hand 1989; Allen 1991; Baas 2004), at flow velocities greater than those required for development of climbing ripples. Additionally, these studies indicate that lamination can be suppressed with high rates of sediment fallout, resulting in the deposition of a massive interval analogous to the Bouma Ta division.

Sandstones with low-angle cross-stratification (facies Scs) compose laminasets ranging from 0.5 to 2 m thick, and display tangentially downlapping foresets. This facies occur filling shallow erosional scours located proximal to the main channel axis, often having abundant clay clasts in the lower foresets. Field relationships show that these facies grade basinward into laminated to massive sandstones, thus suggesting conditions of higher shear stress required for its origin. Facies Scs is interpreted as deposited by the migration of low-relief dunes at the base of an overpassing turbulent flow. The low-angle foreset dipping less than 15° and its almost convex-up shape suggest deposition from a quasi-steady flow with high suspended load (Midtgaard 1996). These dunes and the resulting stratification resemble those generated by Leclair (2002) in a series of flume experiments with an aggradation rate up to 0.014 mm s^{-1}. Leclair (2002) states that flow conditions and sand content used during the experiments allowed both bedload and suspended-load sediment transport. The presence of rounded clay clasts in facies Scs is here related to bedload transport at the base of a long-lived hyperpycnal flow.

Another group of clastic facies includes sandstones related to eolian environments. Eolian facies constitute a minor component in the succession, and generally occur at marginal paleogeographic positions in

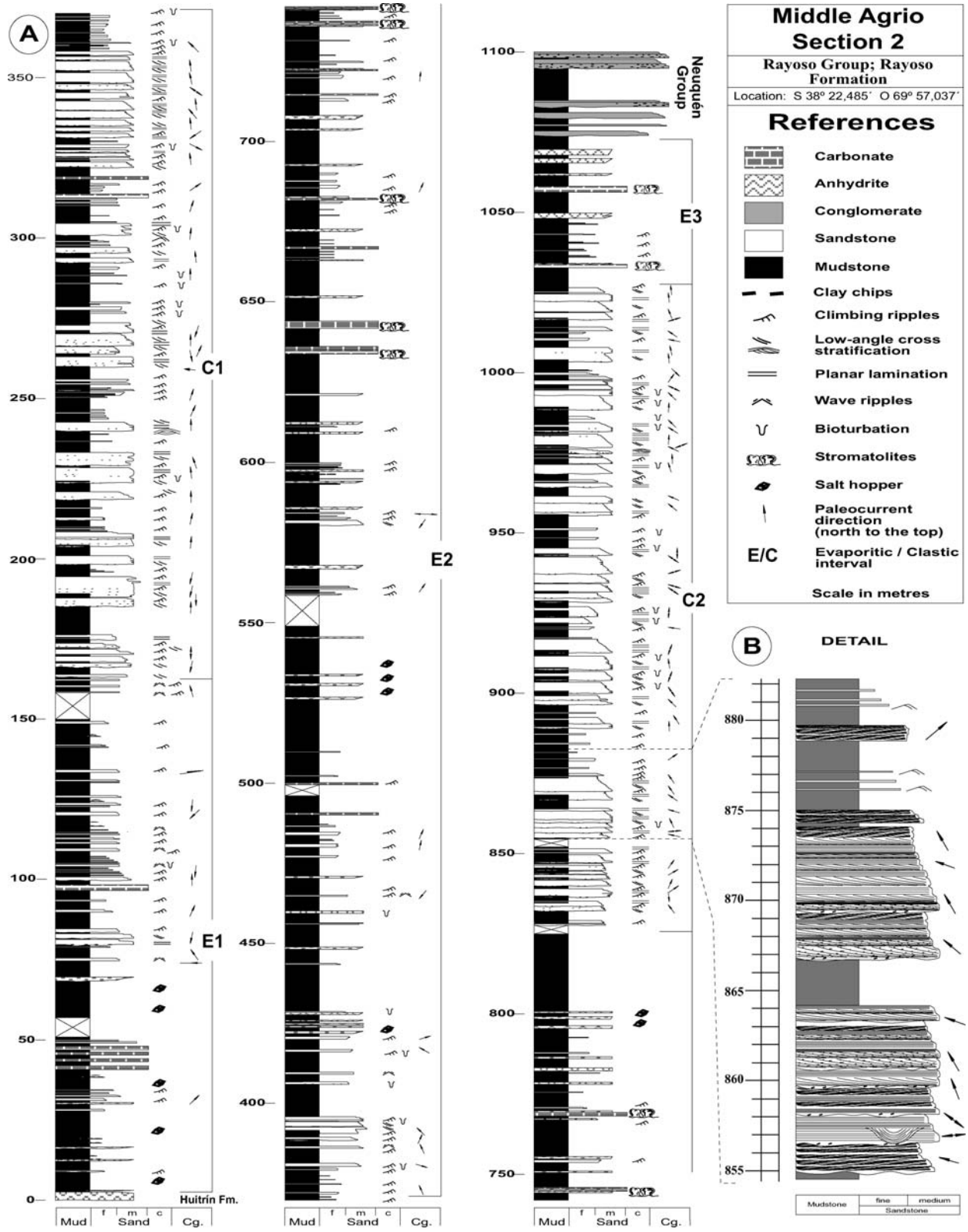

FIG. 4.—**A)** Measured section of the Rayoso Formation at the Agrio del Medio locality (section 2 in Figure 3) showing three evaporitic and two clastic intervals. **B)** Detail of two sandstone bodies of the second clastic interval showing facies recurrence due to flow fluctuations.

TABLE 1.—*Main characteristics of clastic, carbonate, and evaporitic facies recognized in the Rayoso Formation. The relative abundance of each facies in clastic and evaporitic intervals is indicated with C (common), R (rare), and A (absent).*

Facies	Lithology	Sedimentary Structures	Geometry	Origin	Thickness range (m)	Clastic interval	Evaporitic interval
Sm	Fine to medium grained sandstones with clay chips.	Massive.	Tabular to lenticular bodies.	Traction plus fallout from quasi-steady turbulent flows.	0.6–4	C	A
Scs	Fine to medium grained sandstones with clay chips.	Low-angle cross stratification.	Tabular to lenticular bodies.	Unidirectional confined flow with high suspended load.	0.5–2	C	A
Shi	Fine to medium grained sandstones.	Isotropic hummocky cross stratification.	Tabular to lenticular bodies.	Unidirectional current with a sub-ordinate oscillatory component.	0.3–1	R	A
Sl	Fine to medium grained sandstones.	Planar lamination with parting lineation.	Tabular to lenticular bodies.	Traction plus fallout from quasi-steady turbulent flows.	0.4–0.8	C	R
Scr	Fine to medium grained sandstones.	Critical to subcritical climbing ripples.	Tabular to lenticular bodies.	Traction plus fallout from quasi-steady turbulent flows.	0.3–1.5	C	R
Sei	Well sorted fine to medium grained sandstones.	Subcritically climbing translatent strata.	Tabular bodies.	Traction in dry interdunes.	0.7–1	A	R
Sed	Well sorted fine to medium grained sandstones.	Large-scale cross-bedding.	Tabular bodies.	Migration of eolian dunes.	0.6–1	A	R
Sem	Fine grained sandstones.	Massive.	Tabular bodies.	Subaqueous grainfall during eolian duststorms.	0.8–1	A	R
Pl	Mudstones.	Lamination.	Tabular bodies.	Precipitation from prodelta plumes.		C	C
Pm	Mudstones.	Massive.	Tabular bodies.	Decantation.		R	C
Cm	Carbonate mudstone (micritic).	Massive.	Tabular bodies.	Photosynthesis.	< 0.3	A	C
Ce	Carbonates.	Rhythmic laminae.	Tabular bodies.	Algal metabolic activity.	< 0.6	A	C
Eh	Evaporite deposits (halite).	Pseudomorphs, skeletal crystals.	Tabular bodies, individual aggregates.	Precipitation from saturated water bodies.	< 0.6–1.2	A	C
Ey	Evaporite deposits (gypsum).	Laminar, nodular.	Tabular bodies.	Precipitation from saturated water bodies.	< 0.3	A	C

a well-defined situation within the succession (Table 1). These facies are interpreted as follows: (1) laminated sandstones with subcritically climbing translatent strata (facies Sei, Fig. 6A), related to migrating eolian ripples (Hunter 1977); (2) asymptotic large-scale cross bedding (facies Sed) associated with migrating eolian dunes; and (3) massive sandstone beds (facies Sem) with transitional boundaries (Fig. 5F) probably formed by subaqueous grainfall during eolian dust storms in adjacent areas.

The finest-grained facies are composed of laminated mudstones (facies Pl, Fig. 5G) deposited by the fallout of silt, mica, and organic debris from prodelta plumes, and massive mudstones (facies Pm, Fig. 6E).

Carbonates and evaporites also have a definite position within the succession (Table 1 and Fig. 7). Carbonate facies are composed of decimeter-thick highly continuous massive micritic limestone beds (facies Cm), and stromatolitic limestone beds (facies Ce) related to algal and microbial activity (Fig. 8).

Evaporitic facies include laminated and nodular gypsum (anhydrite) (facies Ey) and halite (facies Eh), the last composed of both individual aggregates (crust) and intra-sediment-grown skeletal crystals. These evaporitic facies record precipitation from brines in a supersaturated water body.

Regionally, facies and stratigraphic analysis show the existence of cyclically stacked evaporitic and clastic intervals (Zavala et al. 2001; Ponce et al. 2002), each one hundreds of meters thick (Figs. 3, 4, 7). Field and subsurface studies (Marteau 2002) indicate that these evaporitic and clastic intervals have a regional significance, thus suggesting an allocyclic control on their origin and internal cyclicity. Consequently, these intervals could correspond to specific (paleoclimatic or paleoenvironmental) conditions during the evolution of the Rayoso Formation (Zavala et al. 2001; Ponce et al. 2002). Figure 7 summarizes the characteristics of both clastic and evaporitic intervals.

Clastic intervals are characterized by a thick succession of siliciclastic deposits composed of fine- to medium-grained sandstone beds, interbedded with grayish to reddish mudstone of variable thickness. Sandstone bodies have tabular to lenticular (channelized) geometries, and internally display clay chips and a complete suite of traction-plus-fallout sedimentary structures (facies Scr, Sl, Sm, Scs, and Shi, Table 1). Mudstone intercalations are usually thin, and typically appear deeply truncated by major sandstone bodies. These mudstones could be massive or laminated. No paleosols or rooted horizons were recognized along the entire study area.

Evaporitic intervals, on the other hand, are characterized by a thick succession of cyclically stacked fine-grained deposits, both clastic and evaporitic, with subordinate sandstone beds. Evaporitic intervals probably accumulated in a standing and closed shallow water body, developed under overall arid climatic conditions, with minor peripheral and localized fluvial discharges supplying a small volume of muds and sands (also composing small Gilbert-type deltaic bodies).

Salts were probably incorporated into the water body by groundwater supply (mainly from the dissolution of evaporites from the underlying Huitrín Formation) and then concentrated by intense evaporation. The

→

FIG. 5.—Examples of main clastic facies of the Rayoso Formation. **A)** Fine- to medium-grained sandstone facies with low-angle cross-stratification (Scs) and abundant clay chips grading upward into massive sandstone facies (Sm). In circle a rock pick for scale. **B)** Scs facies. Note the overall climbing and the convex-upward features near the top. 1.8 cm coin in circle stands for scale. **C)** Isotropic hummocky cross-stratification facies (Shi). **D)** Massive sandstones alternating with laminated facies suggesting fluctuations in the fallout rate from the parent flow. **E)** Facies Scr alternating with laminated sandstone facies (Sl) suggesting a fluctuating parent flow. Lighter for scale (7 cm). **F)** Massive sandstone facies of eolian origin (Sem) accumulated by grainfall in a lacustrine body of water. Note that sandstone levels have transitional lower and upper boundaries. A 1.7 cm coin for scale. **G)** Laminated mudstone facies (Pl) deposited by prodelta plumes, 1.7 cm coin for scale.

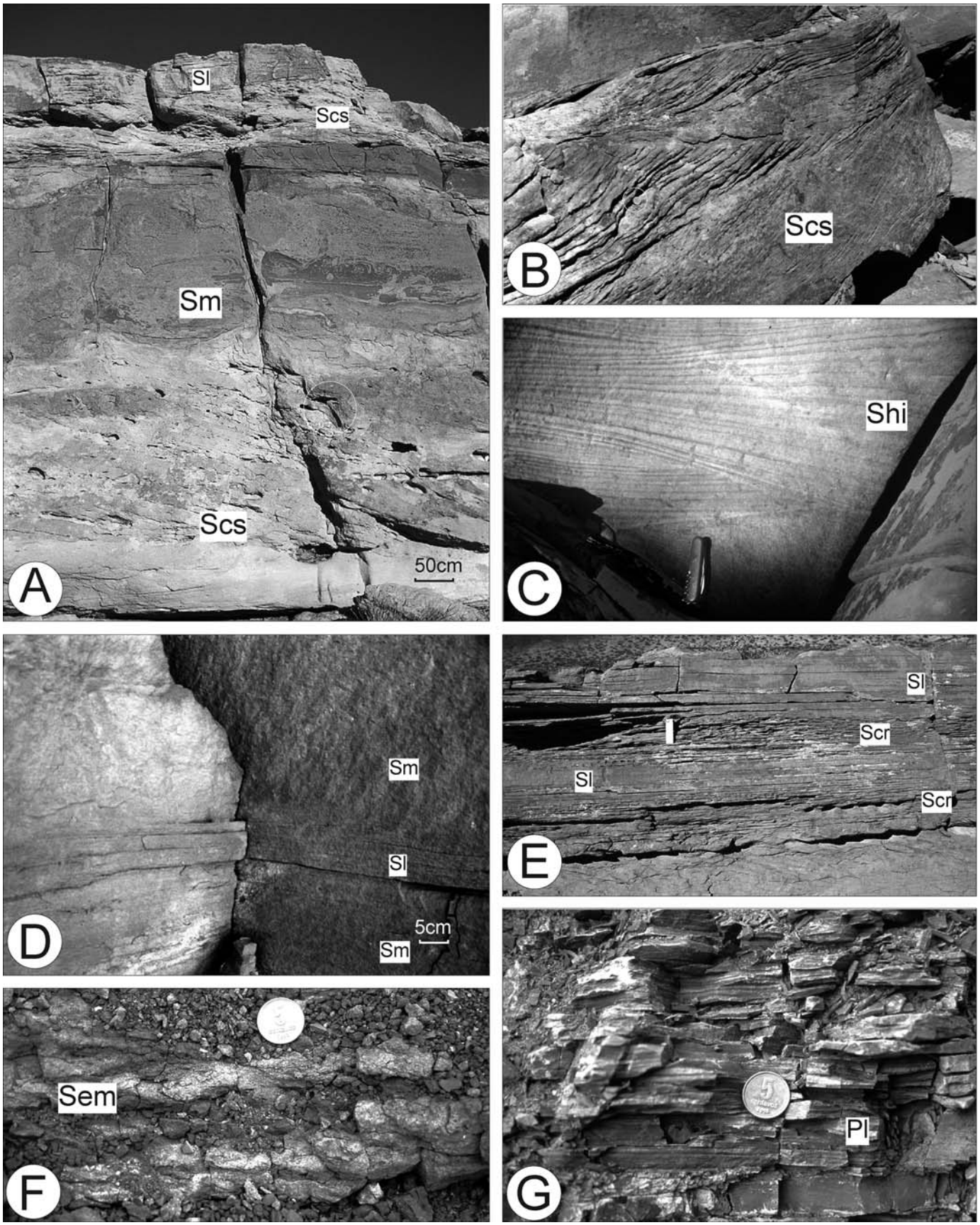
Sl
Scs
Sm
Scs
50cm
A
Scs
B
Shi
C
Sm
Sl
5cm
Sm
D
Sl
Scr
Sl
Scr
E
Sem
F
Pl
G

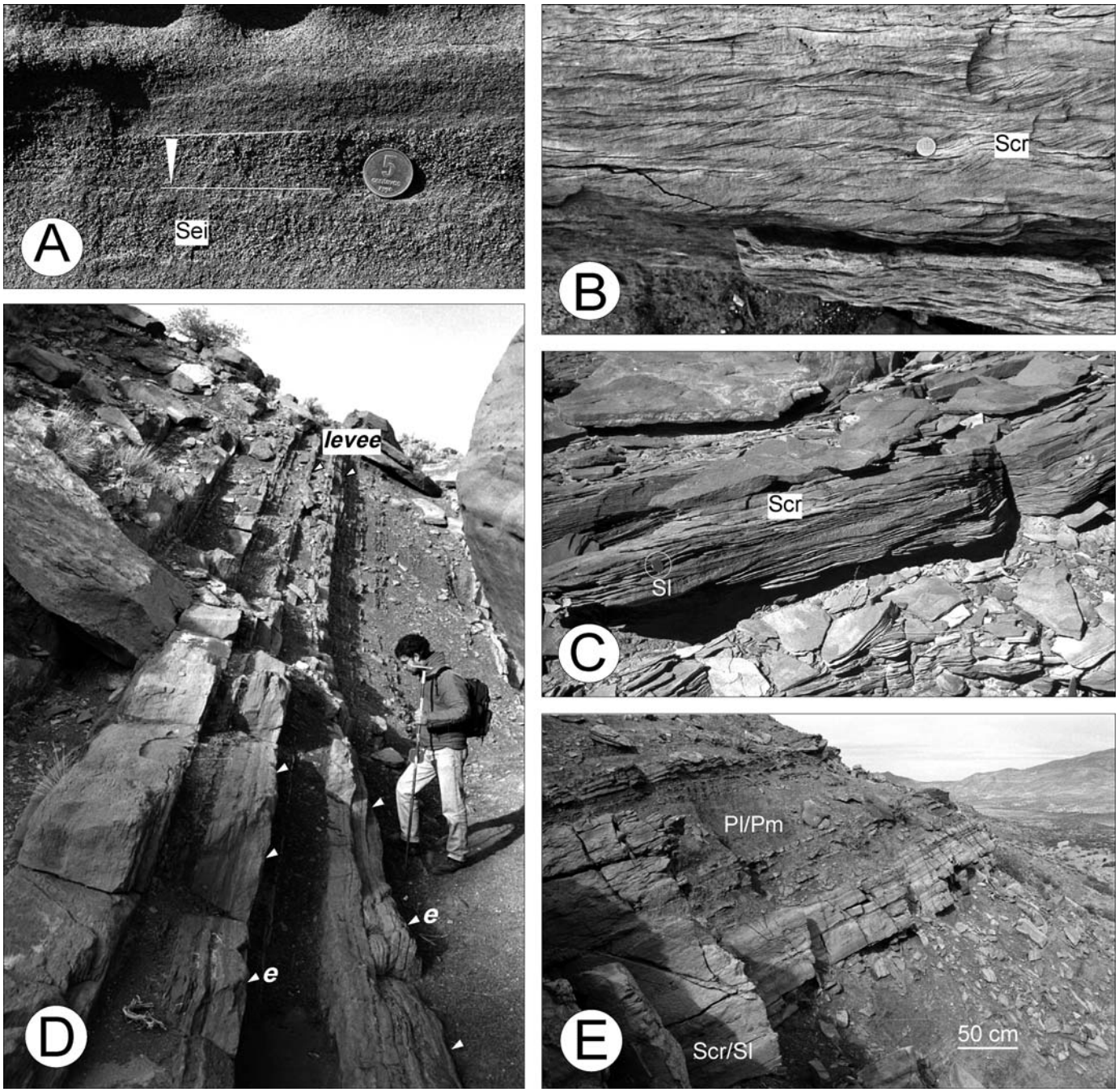

FIG. 6.—Examples of main clastic facies and facies associations of the Rayoso Formation (cont.). **A)** Laminated sandstones of eolian origin (Sei). Note the inverse grading, which is typical of climbing translatent strata; 1.7 cm coin for scale. **B)** Fine-grained sandstones with climbing ripples (facies Scr); 1.7 cm coin for scale. **C)** Alternation of Scr and Sl facies suggesting a progressive deposition from a quasi-steady low-density flow, of fluctuating velocity; 1.7 cm coin for scale. **D)** Detail of the lateral evolution of shallow channelized sandstone bodies. Note how the basal erosional surfaces (e) in the channel axis pass laterally into a concordance in the zone of the subaqueous levee. **E)** Particular view of lacustrine sandstone lobes in more distal positions. Note the overall tabular geometry.

common and cyclical occurrence of stromatolites (Fig. 8) suggests periods of clear waters (with minor content of suspended sediments) of moderate salinity. These organisms probably developed during times characterized by limited clastic supply, and they tend to be absent when minor fluvial systems introduce limited volumes of mudstones to the lacustrine body. Regional distribution of stromatolites also suggests shallow-water conditions for the entire basin, because modern lacustrine stromatolites were reported at a water depth of 15–50 m in lake Tanganyika (Cohen and Thouin 1987) and could extend up to 100 m in lake Van, Turkey (Kempe et al. 1991).

Mudstones in evaporitic intervals contain an association of charophytes, ostracods, small dinoflagellates, palynomorphs, and hypohaline foraminifers characteristic of a lacustrine continental environment (Musacchio and Vallati 2000). These mudstones are often massive or laminated, occasionally

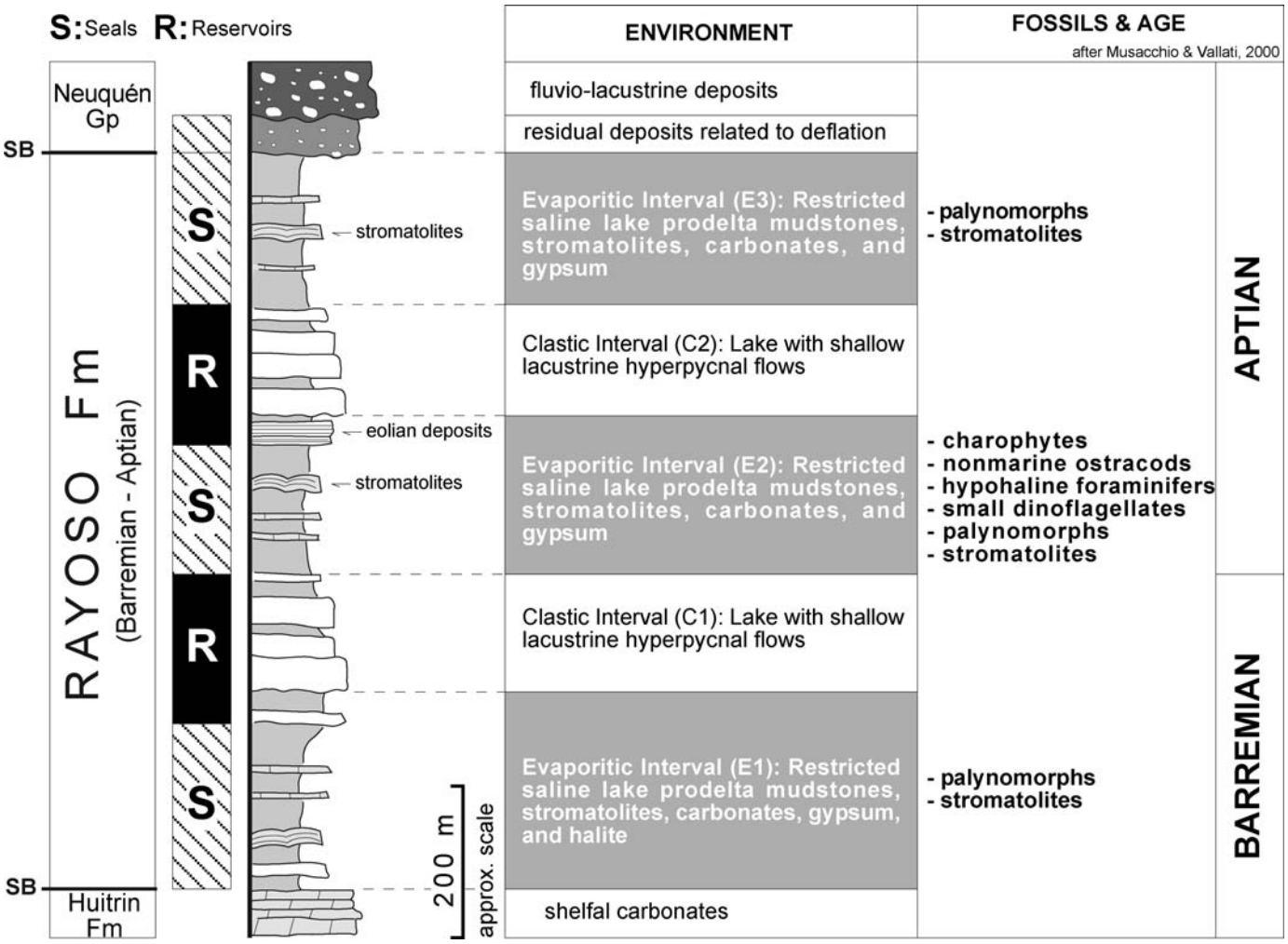

FIG. 7.—Idealized column of the Rayoso Formation (modified after Zavala et al. 2001; Ponce et al. 2002). Note the recurrence of evaporitic and clastic intervals. Paleontologic content and dating inferences are based on biostratigraphic studies by Musacchio and Vallati (2000).

with mudcracks. Mudcracks were recognized only at marginal positions located close to the margin of the paleo-lake, and they were often associated with thin sandstone levels with wave ripples and eolian deposits.

The water body was probably surrounded by large and extended eolian systems, with dunes and associated interdunes of limited preservation (Fig. 9). The existence of these coeval eolian systems are of fundamental importance to justify the nature of the main clastic supply, because they can store a huge volume of fine- to medium-grained sand to be transferred to the basin during the next clastic interval. Consequently, extremely arid periods during evaporitic intervals, with their associated eolian systems, were probably the main "factory" of well-sorted sand constituting present sandstone reservoirs.

FIG. 8.—Stromatolitic limestone bed interbedded in red mudstones within the third evaporitic interval at the Agrio del Medio section (Fig. 4).

Clastic intervals involved more humid periods, where a great volume of sands previously matured in eolian systems during evaporitic intervals were eroded and progressively transferred to the adjacent lacustrine basin by low-gradient fluvial systems. Once reaching the coast, these sediment-laden fluvial discharges would not have produced "normal"-type deltaic systems. According to the relatively high density of these discharges, the flows sank below the lake surface, generating long-lived hyperpycnal flows capable of transporting sand basinward. Additionally, the associated volume of freshwater supply during clastic intervals resulted in a dilution and relative rise of the water body. This dilution and the ensuing transition to a brackish to freshwater lake are also supported by the absence of carbonates and evaporite levels in clastic intervals. The resulting lower density of the receiving water body could favor the generation of hyperpycnal flows also during fluvial discharges having low sediment concentration, and possibly partially suppress the effect of lofting. Flow fluctuations recognized from the analysis of many

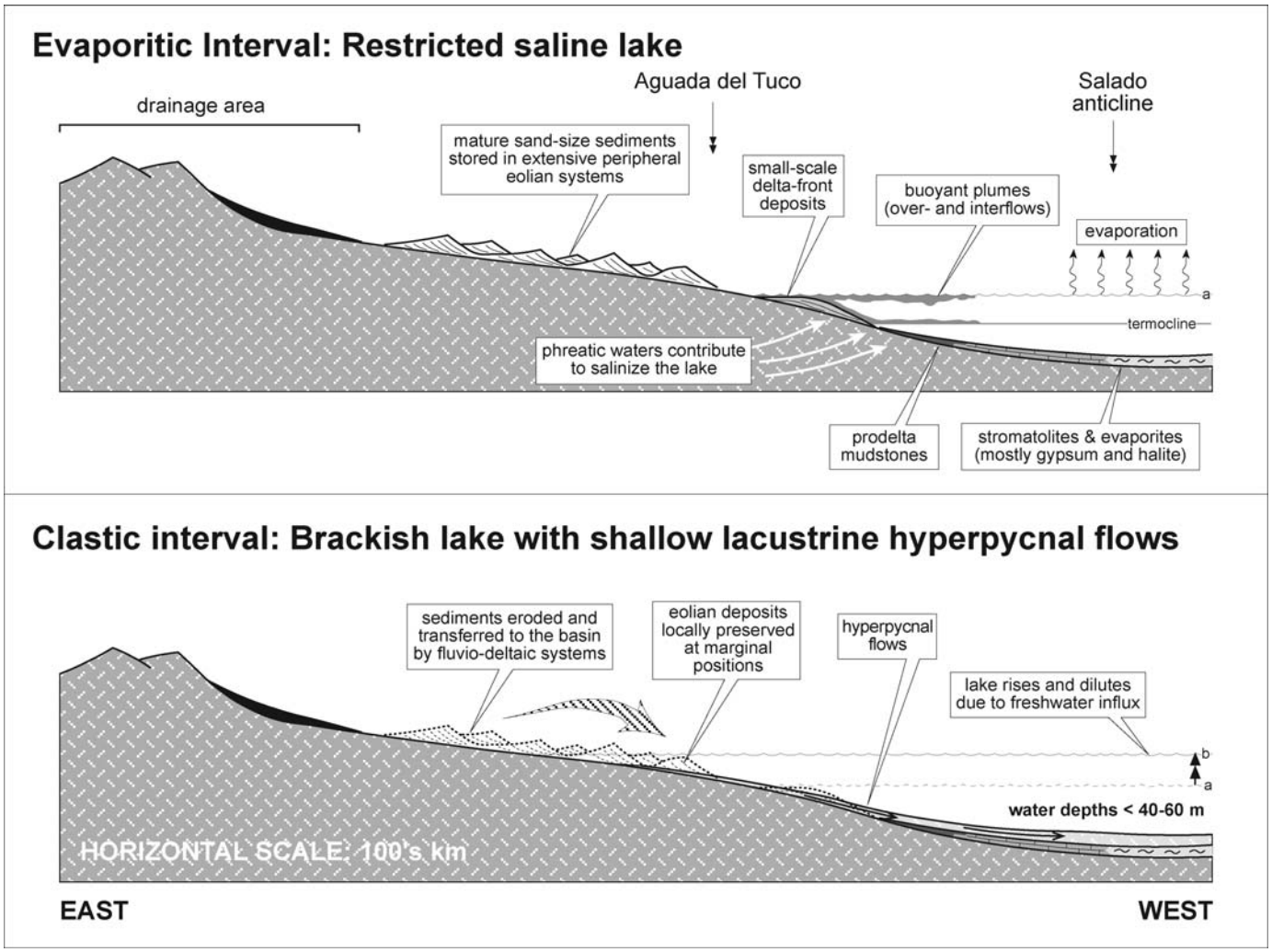

FIG. 9.—Scheme showing main facies associations during both clastic (shallow lake affected by hyperpycnal flows) and evaporitic (shallow and restricted saline lake) intervals. Modified after Zavala et al. (2001) and Ponce et al. (2002).

sedimentary structures within major sandstone beds strongly suggest long-duration flows originated by nearly continuous sustained discharges. These long-sustained discharges (resulting in quasi-steady hyperpycnal flows) allowed these currents to travel tens of kilometers basinward also with very low gradients (i.e., less than 1 m/5 km; Dott 1963). Field and subsurface data support that hyperpycnal flows in the Rayoso Formation have traveled more than 150 km along the bottom of a shallow lake, with no significant textural changes in their associated deposits. Although high velocities can be achieved locally in the body of a hyperpycnal flow, a single hyperpycnal discharge could not travel faster than its related leading head. Because the leading head is characterized by accumulation under traction-plus-fallout conditions (mostly sandy–silty deposits with lamination and climbing ripples), flow velocities are in the order of few centimeters per second. Consequently, to reach a distance of about 150 km, a hyperpycnal flow advancing at an averaged speed of 20 cm s^{-1} requires a discharge maintained during at least 8.7 days. Although these values are highly speculative, they suggest the existence of hyperpycnal discharges lasting for days or weeks for the Rayoso Formation.

River-derived hyperpycnal flows are thought to be the main mechanism responsible for the sand transfer into the basin. Because these deposits often contain large hydrocarbon accumulations (Marteau 2002), the analysis and understanding of the main characteristics of these sandstone bodies (textural and facies changes, extension, geometry, and continuity) are of fundamental importance for the development of present and future petroleum reservoirs on this and other similar depositional units.

Although the hydrodynamic evolution of these long-duration hyperpycnal flows are at present poorly understood (Mulder and Alexander 2001a; Gani 2004), the excellent field exposures of the Rayoso Formation allow us to explore some new concepts based on the analysis of facies relationships observed in the field. The theoretical framework discussed below proposes a mechanism to explain how poorly channelized sandstone bodies could extend tens of kilometers basinward without displaying significant textural changes in their associated deposits.

TRACTION AND TRACTION-PLUS-FALLOUT STRUCTURES

Numerous flume experiments carried out during the past four decades (e.g., Simons et al. 1965; Southard 1991) have documented the direct association between tractional sedimentary structures and sediment-free water flows in alluvial channels. Results show that a water stream, moving over an unconsolidated sand substrate, generates different kinds of bedforms on the lower interface, which are stable forms that mainly depend on the grain size, depth, and velocity of the water flow (among

other parameters such as fluid density, temperature, etc.). As an example, water moving over fine-grained sand generates ripples, dunes, plane bed, and finally antidunes as velocity increases (Simons et al. 1965; Southard 1991). Although these papers clearly stated that the bedform succession generated during these flume experiments apply only for open channels, their related succession of sedimentary structures were often used to analyze turbidites. Arnott and Hand (1989) and Shanmugam (2000) noted that the succession of sedimentary structures generated by a waning clear-water flow moving above fine-grained sand in flume experiments (open channels) differs from those of the Bouma sequence, and concluded that they may not accurately represent conditions beneath turbidity currents characterized by abundant rain of sand-size sediment from suspension.

To analyze the deposition from sediment-laden hyperpycnal flows it is necessary to discuss the accumulation under traction-plus-fallout conditions. Water flows in open channels are fluid gravity flows, and the bedforms generated over a sandy substrate are mainly a consequence of drag and frictional forces. In contrast, hyperpycnal flows are sediment gravity flows composed of different mixtures of water and sediments, and deposition occurs mostly under traction-plus-fallout conditions. These traction-plus-fallout conditions generate a complete suite of sedimentary structures, which are often confused with those produced by sediment-free water flows. A particular case of this confusion has been noted early by Sanders (1965), who compared the origin of parallel laminae originated in a flume experiment with clear water, with that related to traction-plus-fallout processes in natural turbidity currents.

In recent years, flume studies were conducted to deeply analyze deposition and sedimentary structures generated in aggrading beds with different amounts of sediment fallout (Banerjee 1977; Arnott and Hand 1989; Storms et al. 1999; Alexander et al. 2001; Leclair 2002), complemented also by numerical approaches (Baas 2004). These studies indicate that most facies originated under traction-plus-fallout conditions are structureless, or display low-angle cross-stratification, parallel lamination, and/or climbing ripples. Nevertheless, flume studies must be applied with caution to the analysis of natural environments, where water depth and outer flow thickness are very much greater. Additionally, flume runs have by now technical limitations in maintaining high aggradation rates for time periods greater than several minutes (Arnott and Hand 1989; Leclair 2002).

Field studies carried out on sandstone bodies of the Rayoso Formation, mostly analyzing lateral (downcurrent) facies evolution along certain levels, indicate that a decelerating hyperpycnal flow under conditions of traction-plus-fallout generated a sequence of sedimentary structures starting with low-angle cross-stratification, followed by massive and/or laminated sandstones, and ending with climbing ripples. This succession seems to apply to an idealized simple waning flow. More commonly, individual sandstone beds in the Rayoso Formation display some departures in the vertical succession of structures. For example, many beds start with transitional or sharp (non-erosional) bases, and internally show a cyclical recurrence of different sedimentary structures (Fig. 4B), suggesting fluctuations in the velocity and/or fallout rates from the parent flow during deposition. Figure 10 shows an example of a single bed thought to be deposited from a fluctuating turbulent and long-duration hyperpycnal flow. In the figure, transitional and repeated passages between sandstones with climbing ripples (facies Scr) and parallel lamination (facies Sl) are related to the progressive growth of the deposit surface during the passage of a relatively long-lived fluctuating flow (for additional examples see also Figs. 5E, 6C).

Deposition under traction-plus-fallout conditions is limited by an erosional velocity threshold, because velocity increase stimulates erosion and higher capacity of the flow to transport suspended sediments (van den Berg and van Gelder 1993). Consequently, once this threshold is achieved, the flow is capable of incorporating previously accumulated material through substantial erosion of its substrate. The value of this erosional threshold is highly variable and depends on the volume of suspended sediment and the type and consolidation of the substrate (among other variables).

FIG. 10.—Close-up of a sandstone bed interpreted to have been deposited by a fluctuating hyperpycnal flow. The gradual passages between Scr and Sl facies is related to velocity fluctuations affecting the overpassing turbulent flow.

AN ACCUMULATION MODEL FOR HYPERPYCNAL FLOWS

Recent experimental studies coupled with some outcrop examples have allowed an outline of some characteristics of deposition by long-lived quasi-steady underflows (or hyperpycnal flows), which in turn provides useful tools to differentiate these deposits from those accumulated by surge-like (or episodic) flows. On slopes of less than 1°, episodic turbidity flows such as those generated from slumps have a tendency to come to rest rapidly, because the short-lived source inhibits the continuous sediment supply of the head, thus enhancing the frictional effect (Kersey and Hsu 1976; Britter and Linden 1980). On the other hand, sustained turbidity flows, generated by hyperpycnal flows at river mouths, tend to be maintained as long as the high-density fluvial discharge continues (Prior et al. 1987). Consequently, the distance reached by hyperpycnal flows is dependent more on the duration of the flood event than on the slope of the system considered. The last explains how river-related hyperpycnal flows could travel across the entire length of Lake Mead (more than 150 km) with a regional slope of less than 20 cm/km (Dott 1963). Other substantial differences can be recognized in the way and position where each flow deposited its load. In surge-like flows deposition is dominated by the head, whereas in hyperpycnal flows deposition is dominated by the body (de Rooij and Dalziel 2001; Peakall et al. 2001). This allows the preservation in the hyperpycnal deposit of evidence of flow fluctuations that occurred during discharge. Finally, flume studies show that episodic flows display a reduced depositional area located immediately downstream of the source area. Conversely, long lived hyperpycnal flows tend to develop a more extensive deposit, with more subtle textural changes (de Rooij and Dalziel 2001).

As expressed above, many sandstone beds of the Rayoso Formation show internal evidence of fluctuations in the velocity and fallout rates from the parent flow indicated by gradual facies changes, which suggest the existence of quasi-steady currents. Figure 11 illustrates a hypothetical velocity curve for a quasi-steady hyperpycnal flow, which is introduced with the purpose of discussing sedimentation from a long-lived underflow at a fixed point. In Figure 11, the upper curve shows the evolution of flow velocity (vertical) with time (horizontal). On the left, a series of critical velocities are indicated. From bottom to top, these velocities are: (1) the interruption of clay settling and passage into the nondepositional field

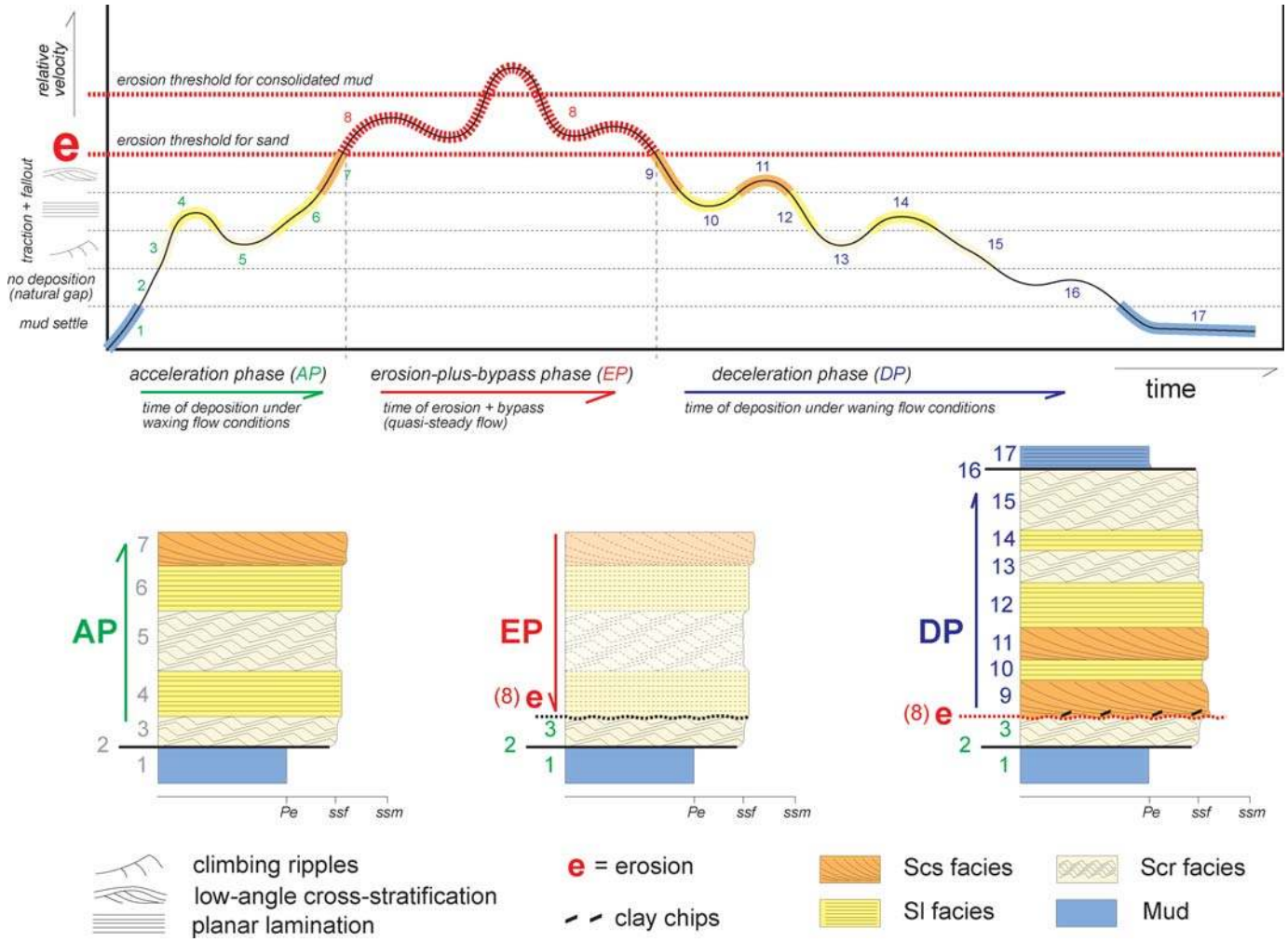

FIG. 11.—Hypothetical diagram showing a curve of fluctuating velocity related to a quasi-steady underflow and its consequences for sedimentation at a fixed point in the basin. Three main phases are recognized: Acceleration phase (AP): accumulation of intervals 1 to 7 by an accelerating and fluctuating flow. Erosion-plus-bypass phase (EP): erosion of some of the preceding deposits. Deceleration phase (DP): accumulation of intervals 9 to 15 from a decelerating and fluctuating flow.

(natural gap), (2) the beginning of deposition under traction-plus-fallout conditions with their corresponding sedimentary structures, and (3) the erosional thresholds (e) for unconsolidated sand and consolidated mud, from which erosion plus transport started. From the analysis of this hypothetical curve for quasi-steady underflows, three main phases can be recognized: *acceleration, erosion plus bypass*, and *deceleration*, each one characterized by a distinctive facies succession. For the following discussion of the internal evolution of these phases, refer to the intervals indicated with numbers (1 to 17) both on the hypothetical curve and on the schematic sections (Fig. 11).

Acceleration Phase (AP)

The acceleration phase (AP) starts over basal mud deposits accumulated during previous events (1). As a consequence of the arrival of a hyperpycnal flow (leading head), velocity progressively increases. Once the natural gap is exceeded (2), this flow in constant acceleration starts to generate traction-plus-fallout bedforms and related sedimentary structures. Under these conditions, a vertical facies succession is generated and composed of climbing ripples (3) followed by planar lamination (4) as the bed shear stress rises. If the underflow velocity fluctuates (flow pulsing), deposition could alternate between climbing ripples and planar lamination (5–6), ending with low-angle cross-stratification (7), thus characterizing currents with velocities located close to the erosional threshold for sands (e).

Erosion-Plus-Bypass Phase (EP)

Once the underflow velocity achieves the threshold for sand erosion, the flow starts to entrain the sand deposits (8) accumulated during the preceding AP phase. The magnitude of this erosion depends on the time that the flow remains in the erosion-plus-bypass phase (EP). If the duration of the EP phase is brief, then the deposits accumulated during the AP phase is partially preserved (as indicated in Fig. 11). On the other hand, if the velocity of the flow is maintained above the erosional threshold for a long time, then the preceding deposits could be totally eroded and redeposited at more distal locations. Finally, if the velocity of the hyperpycnal flow exceeds the threshold for the erosion of consolidated mud, the flow is capable of incorporating clay chips from the pre-event bed. According to its erosive characteristics, the existence of this phase is fundamental for the generation of channelized bodies. Although in the example shown in Figure 11 a simple EP phase is illustrated (with a single erosional surface), in field examples the existence of multiple erosional surfaces within individual event deposits is very common, suggesting velocity fluctuations above and below the erosional threshold.

Deceleration Phase (DP)

The deceleration phase (DP) is caused by a decrease (or fluctuating waning) of flow velocity within the traction-plus-fallout deposition zone, until it is completely deactivated (zero velocity). Sedimentary structures during the DP often record minor fluctuation in the decelerating flow (9 to 15). These deposits often include clay chips, which are indicative that flow velocities in the upcurrent direction have exceeded the erosional threshold of consolidated mud (especially during EP phase). In the final stages of deceleration, the flow velocity falls into the natural gap area (16) characterized by no sand deposition, and finally ends with the accumulation of mud, suggesting the complete deactivation of the flow.

BASINWARD EVOLUTION OF HYPERPYCNAL SYSTEMS

The model discussed above applies to a hypothetical hyperpycnal flow evolution at a fixed position within the basin. The analysis of contemporaneous flow evolution at different basin locations provides a further understanding of some distinctive characteristics of hyperpycnal-flow sedimentation. Figure 12 depicts this relationship from a hypothetical example, relating velocity with time. The three curves shown in Figure 12A represent the variation of one flow with time at different basin positions. The black curve corresponds to proximal positions (I), the gray curve to intermediate ones (II), and the dashed curve to distal sites (III). The case discussed here involves the downslope temporal evolution of a fluctuating hyperpycnal flow and the consequences for sedimentation, not only in the nature and geometry of the related deposits but also in the generation of erosional surfaces. The plan scheme in Figure 12B shows the relative position of the river mouth (heavy lines on the left) and the location of zones I, II, and III. In this scheme the relative velocities vary with distance from the flow axis, e.g., flow velocity reaches its maximum at the axial zone and diminishes progressively towards the flanks. Both the velocity curves in Figure 12A and the longitudinal sections (Fig. 12C) represent velocity changes and erosional or depositional processes that apply to the axial zone. In order to discuss the basinward evolution of a fluctuating hyperpycnal flow with time, several situations will be considered.

The first longitudinal section shown in Fig. 12C (belonging to time t_1–t_2) illustrates the initial sedimentation (overall waxing; black and gray curves), once the critical threshold of nondeposition is exceeded. Under these conditions, sedimentation starts on proximal (I) and intermediate (II) zones with sand deposits having climbing ripples, parallel lamination, and low-angle cross-stratification, respectively, which are characteristics of an AP phase. During this first considered span of time the hyperpycnal flow has not reached the distal zone (III). The maximum velocities developed during this first stage in zones I and II do not exceed the erosional threshold (e), thus resulting in the accumulation of tabular graded beds with transitional or sharp bases (lobes) without erosional features.

At time t_3 the flow velocity, affected by a progressive and continuous acceleration, is above the erosional threshold at proximal zones (I) producing channelization (EP phase). Flow velocities at intermediate zones of the basin (II) are still below the erosional threshold, that is, within the transport-plus-fallout deposition area, and thus characterized by the deposition of climbing ripples, parallel lamination, low- angle cross-stratification, and all the variations produced by flow fluctuation during an AP phase. At the same time, more distal positions (III) are still dominated by normal mud settling. This situation is characterized by the construction of vertical facies sequences starting with erosional bases at proximal positions, and transitional to sharp bases at more distal zones.

During time t_4, at both proximal (I) and intermediate (II) zones, the flow has velocities that exceed the erosional threshold. Under these conditions, erosion continues at proximal zones (I) while intermediate zones (II) start to be affected by the erosion of previously accumulated sediments (EP phase). Towards more distal positions (III) flow velocity has reached the range of traction-plus-fallout deposition, thus resulting in the deposition in AP phase of sandstone levels with climbing ripples and parallel lamination.

The span of time t_1–t_4 is then characterized by a basinward shift in facies produced by a progressive and constant system advance. Consequently, flows gradually pass from AP to EP phases, resulting in a progressive advance of channelized areas towards the basin center. This results in a poor preservation of deposits formed during the advance stage, especially in the axial flow zone.

During the span of time t_5–t_7 the three velocity curves are within the transport-plus-deposition zone, with a continuous decrease in velocity. Consequently, this situation is characterized by sand deposits with traction-plus-fallout structures within a DP phase, which often passively infill the erosional topography previously generated at proximal areas. As a consequence, in distal areas sedimentation occurs over a relatively flat topography and deposits acquire a lobate geometry. At proximal positions, sandstones with similar grain size and sedimentary structures infill channelized features. If the DP phase is relatively long, channels may be filled completely with simple or complex (with lateral accretion) sandstone bodies. On the other hand, if the DP phase is brief, proximal channels may be either partially filled by sand, or be mud-draped (Fig. 13).

The preceding discussion concerning depositional phases at different positions in the basin for quasi-steady sand-rich hyperpycnal flows is fundamental to justify the great lateral extent of sandstone bodies without significant textural changes as observed in the Rayoso Formation, and the coexistence of erosion and depositional processes at the same time along with the extension of an individual flow. In most hyperpycnal flows the coexistence of erosional and depositional processes can be recognized between the center and the lateral parts of the flow at channelized proximal areas, with important consequences concerning geometry and lateral extent of sandstone bodies.

Figure 14 shows a series of schemes (on the right) for the evolution of a hyperpycnal flow and the consequence for sedimentation (right) by means of a series of transversal sections at certain zone indicated as A–A′.

Diagrams (1) correspond to the AP phase. The flow displays maximum velocities in the axial zone, which progressively decreases both laterally and distally. As a consequence of having achieved the erosional threshold, flow velocity in the axial zone produces an incipient and elongated erosional depression in proximal areas (indicated in the figure by light gray). At this moment, in the zone of the transverse section A–A′, flow velocities are relatively low, resulting in the deposition of relatively tabular beds (lobes) containing traction-plus-fallout sedimentary structures deposited under the AP phase.

During EP phase (2) the system experienced the maximum advance of subaqueous channels. As a consequence in the zone of the section A–A′ the flow has produced some erosion on the previously deposited frontal lobe at the axial zone, while towards the lateral parts the existence of lower velocities results in the deposition of thin levels of subaqueous levee.

Finally, during the DP phase (3) the overall waning flow results in the deposition of its suspended load (in the case of the Rayoso Formation up to medium-grained sands) with similar grain size in both proximal (here infilling erosional depressions) and distal areas. Consequently, in the section A–A′ the final channel fill has some typical and diagnostic characteristics that differentiate it clearly from subaerial channels. One of these characteristics is that erosional surfaces tend to predominate towards the channel axis, and progressively disappear towards the lateral areas, where they become sharp or transitional boundaries. One example of these lateral changes could be observed at the detailed section of Figure 15 and in Figure 6D. Another difference resides in the fact that levee deposits associated with hyperpycnal flows show paleocurrents oriented up to 45° to those of the axial flow direction (Remacha et al. 1994; Dutton et al. 2003), while levees associated with subaerial channels (because of their origin

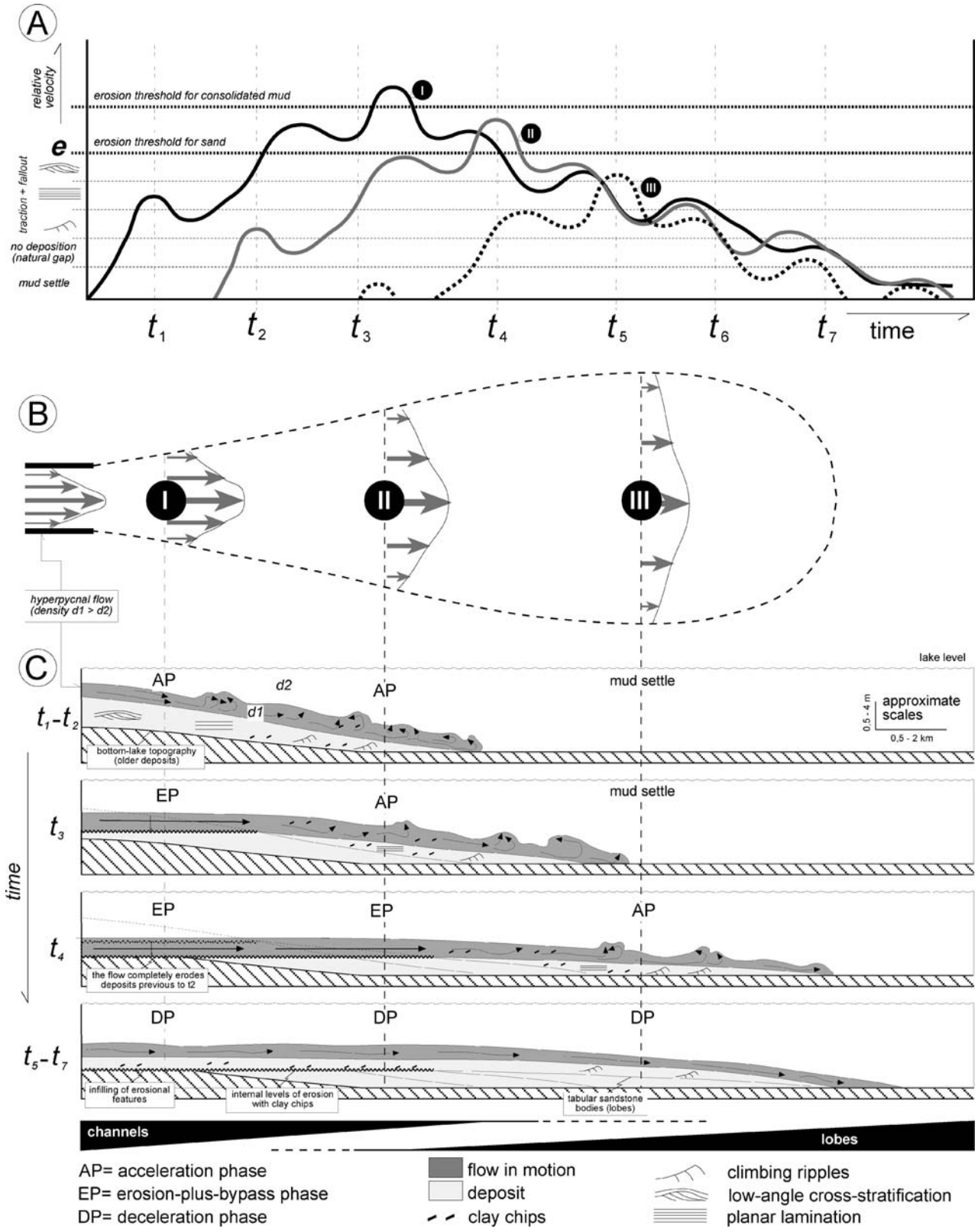

FIG. 12.—Hypothetical diagram showing the temporal evolution of a quasi-steady flow and related deposition at different positions within the basin with time. **A)** The three curves indicate flow variations for the three different locations. Black curve: proximal zone or "I." Gray curve: intermediate zone or "II." Dashed curve shows distal zone or "III." **B)** The two former longitudinal sections (time t_1–t_3) illustrate the initial sedimentation. Sedimentation starts on proximal (I) and intermediate (II) zones, while the distal zone (III) has not yet been reached for the flow. **C)** (time t_4) illustrates the conditions with erosion at the proximal location and deposition in the distal (III) one. The last longitudinal section shows the conditions during final stage characterized by deposition over the entire area.

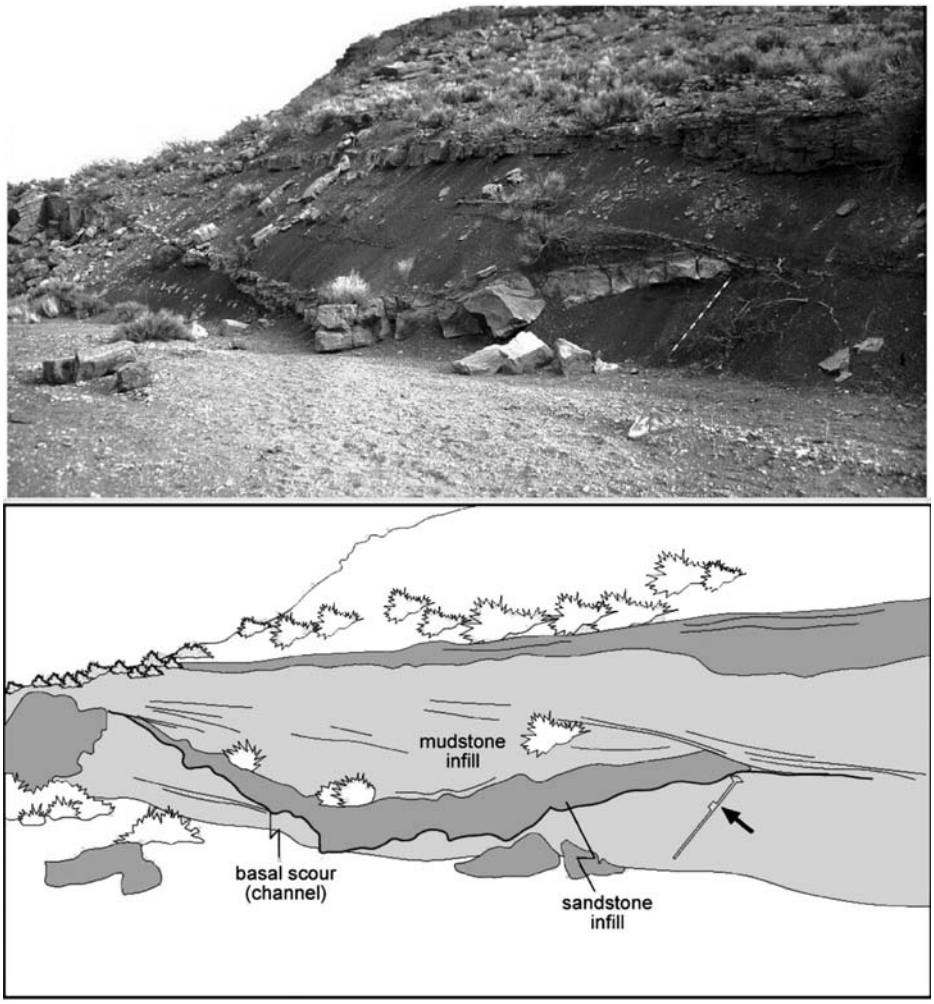

FIG. 13.—View (top) and line drawing (bottom) of a partially filled small channel produced during the EP phase. This partial infill could be related to a rapidly decaying velocity associated with a relatively brief DP phase. Black arrow indicates the scale (Jacob's staff).

related to overflow) often display paleocurrents oriented at higher angles. Additionally, levee deposits in hyperpycnal system often disposed over the frontal lobe accumulated during the early AP phase. The incision of the frontal lobe caused by the advancing related channel was recently documented in flume studies (Métivier et al. 2005).

Because velocity changes in hyperpycnal flows occur not only along the flow axis but also towards the flanks, facies changes do so as well (Figure 16). Consequently, detailed facies analysis in the transition between channel axis and levees is fundamental to document and predict the main facies family expected to occur in the hyperpycnal system along kilometers in a longitudinal section.

DISCUSSION

Because hyperpycnal systems are the subaqueous extension of subaerial fluvial systems, they keep some characteristics typical of fluvial deposits (e.g., channels, flow fluctuations, meandering, bedload, etc.). Consequently, distinguishing between subaerial fluvial deposits and lacustrine hyperpycnites is not always a simple task, because their differences can be very subtle.

The main characteristics that allow the recognition of ancient lacustrine hyperpycnites can be summarized as follows: (1) the dominance of sedimentary structures related to traction-plus-fallout processes in sandstone bodies, which indicate a flow with a high suspended load; (2) the vertical recurrence within a single sandstone bed of facies related to different hydrodynamic conditions, which suggests fluctuations in the flow energy related to a long-lived fluvial discharge; (3) the occurrence of discontinuous erosional surfaces within single sandstone beds, because the existence of coeval erosional and non-erosional surfaces is a distinctive feature of hyperpycnal deposits; (4) the presence of very thick sandstone bodies (more than 4 m thick) related to gradual deposition from a single sustained flow, thus suggesting an excess of accommodation space during deposition, which is more common in subaqueous environments; (5) the existence of regionally extensive clastic successions hundreds of meters thick (coarse-grained channel fills, tabular sandstone bodies and mudstones) not confined in valleys, indicating a widespread accumulation in the depositional zone rather than in the transfer zone (Schumm 1981); (6) the lack of evidence of reworking by sediment-free water flows within sandstone bodies, because hyperpycnal flow are typically sediment gravity flows without a final clear-water stage. Additionally, the absence of paleosols and mudcracks supports the interpretation at a subaqueous environment, and definitive evidence is provided by the presence (if any) of associated lacustrine microfossils and stromatolites.

Because hyperpycnal turbidity currents may have a longer duration and greater steadiness than surge-like turbidity flows, their deposits are likely to be significantly different (Alexander and Mulder 2002). Although deposits related to surge-like flows have received great attention during the last decades, the understanding of facies and

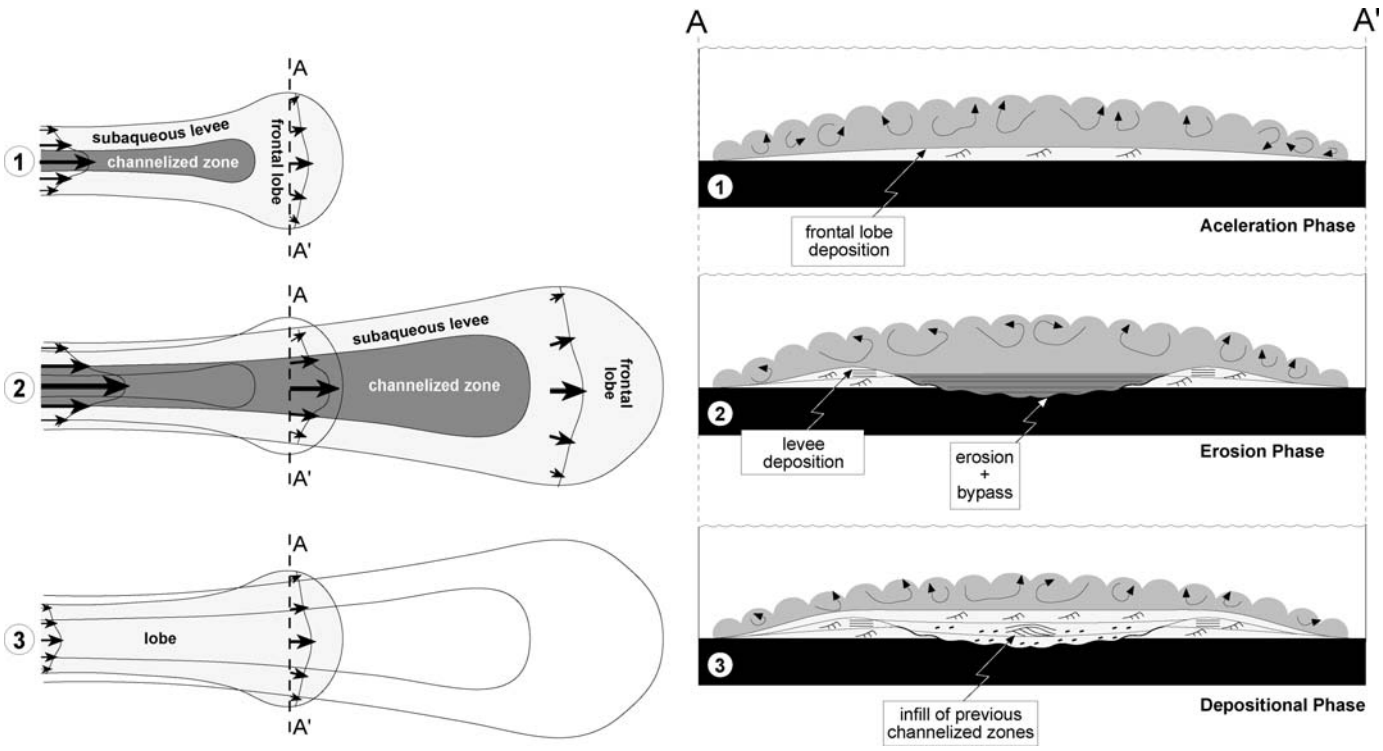

FIG. 14.—Plan view (on the left) of the evolution of a quasi-steady hyperpycnal flow and their consequences in the lateral geometry of the deposits (right). Note in 2 the coexistence at the same time of erosion at the channel axis and deposition in the laterals (levees).

facies relationships related to sustained hyperpycnal flows is still in its infancy. According to the current paradigm, especially after the excellent contribution of Bouma (1962), it is generally thought that sandstone facies having climbing ripples (Bouma division Tc) are characteristic of medium to distal depositional areas, and that no substantial sandstone deposits are expected to exist basinward of this point. This paradigm probably applies mostly to surge-like and consequently highly discontinuous turbidity flows. The depositional model for sustained hyperpycnal flows induces a substantial modification to the last paradigm, because it can adequately explain how fine-grained sandstones (for example, having climbing ripples) could exist at the same time in both proximal and distal areas, along distances of tens of kilometers. Consequently, the determination of the relative position of sandstone deposits within the basin cannot be made only according to the types of sandstone facies, but also considering the existence of internal erosional surfaces.

Even though the depositional model here discussed was built from the analysis of lacustrine strata, we consider that the main concepts could also be applied for the understanding of shallow and deep marine hyperpycnites. Although sandy hyperpycnites and classical (surge-like) fine-grained turbidites (Bouma 2000) could potentially be confused according to some similarities (specially if there is a lack of data), they have differences, and it could be impossible to separate them without careful studies (A. Bouma, personal communication).

CONCLUSIONS

The Cretaceous Rayoso Formation in western Argentina comprises a sedimentary unit up to 1200 meters thick that is widely distributed in the Neuquén Basin. The analysis of major sandstone bodies reveals deposition from sustained hyperpycnal flows in a shallow perennial lake.

Deposits related to hyperpycnal flows are composed of sandstone beds having tabular to lenticular geometries and internally show a dominance of traction-plus-fallout structures. Facies within single sandstone beds display a gradual recurrence of sedimentary structures related to different flow conditions, thus suggesting deposition from a fluctuating flow. Although retrogressive slumping could sustain turbidity currents over a period of many hours (Piper et al. 1999), the existence of long-lasting (days or weeks) fluctuating flow is here considered a diagnostic feature that indicates a fluvial connection.

The analysis of single hyperpycnites at a fixed point reveals the existence of three depositional phases, here called *acceleration (AP)*, *erosion-plus-bypass (EP)*, and *deceleration (DP)*, which record the complete evolution of a single sustained hyperpycnal flow. The *acceleration* phase starts with the arrival of a sustained hyperpycnal flow, and is characterized by the deposition of traction-plus-fallout sedimentary structures that can record flow fluctuations during an overall acceleration. Once the velocity exceeds the erosional threshold, during the *erosion-plus-bypass* phase, the flow starts to erode and transport the sandstone deposits accumulated during the preceding phase. The *deceleration* phase is related to a fluctuating decrease in flow velocity until its complete termination, and is characterized by the deposition of traction-plus-fallout sedimentary structures filling the erosional surfaces produced during the previous phase.

The depositional evolution of a single long-lived hyperpycnal flow with distance records initially the progressive basinward migration of the AP and EP phases, and finally an overall deposition under the DP phase both in proximal and distal areas. This evolution provides an adequate explanation for the basinward extension of channelized

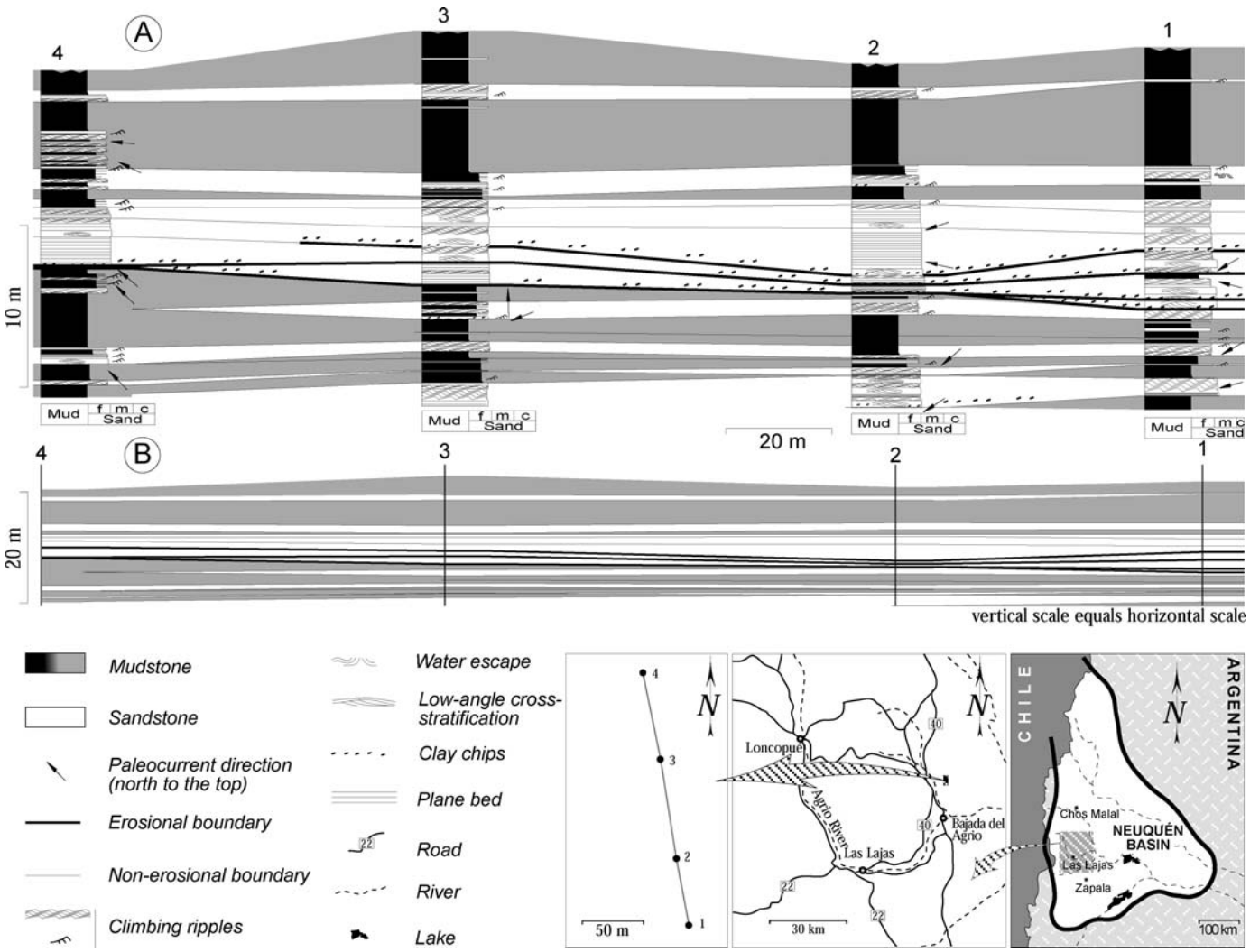

FIG. 15.—**A, B)** Detailed cross section on a subaqueous channel in a direction roughly perpendicular to the paleoflow. Note the existence of numerous erosional surfaces draped by clay chips near the channel axis (section 2) and how these erosional surfaces change laterally into sharp or transitional facies boundaries (section 4).

features, and for the occurrence of fine-grained sandstones with climbing ripples both in proximal and distal positions within the same hyperpycnal system. Consequently, facies analyses derived from application of the Bouma sequence do not apply to quasi-steady hyperpycnal flows.

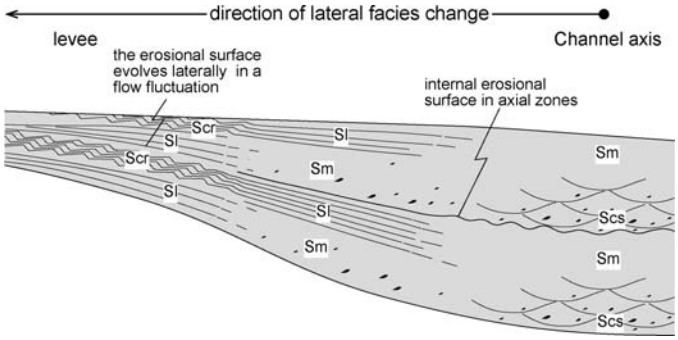

FIG. 16.—Diagram showing facies changes between channel axis and levees. Consequently, detailed facies analysis in the transition between channel axis and levees is fundamental to document and predict the main facies family expected to occur in the hyperpycnal system along several kilometers in a longitudinal section.

ACKNOWLEDGMENTS

The writers deeply acknowledge the unselfish backing of Jan Alexander (University of East Anglia) who read an earlier version of this paper. Field discussions with Stephen Molyneux, Chris Forster (EnCana UK Ltd) and Augusto Silva Telles (Petrobras) have really helped to improve this work. The present work would not have been possible without the field collaboration of Gustavo Azúa. Marcelo Marteau (Petrobras) has also aided in the research by carefully studying the subsurface. We are grateful to the CONICET and the Geology Department of the Universidad Nacional del Sur for their continuous support. Extensive review and constructive comments from Richard Yuretich, Peter Drzewiecki, Jan Alexander, and Colin P. North, together with suggestions from Arnold Bouma and John B. Southard, have helped to greatly improve this manuscript. Emilano Mutti is always present inspiring our research group.

REFERENCES

ALEXANDER, J., AND MULDER, T., 2002, Experimental quasi-steady density currents: Marine Geology, v. 186, p. 195–210.

Alexander, J., Bridge, J.S., Cheel, R.J., and Leclair, S.F., 2001, Bedforms and associated sedimentary structures formed under supercritical water flows over aggrading sand beds: Sedimentology, v. 48, p. 133–152.

Allen, J.R.L., 1991, The Bouma division A and the possible duration of turbidity currents: Journal of Sedimentary Petrology, v. 61, p. 291–295.

Arnott, R.W.C., and Hand, B.M., 1989, Bedforms, primary structures and grain fabric in the presence of suspended sediment rain: Journal of Sedimentary Petrology, v. 69, p. 1062–1069.

Banerjee, I., 1977, Experimental study on the effect of deceleration on the vertical sequence of sedimentary structures in silty sediments: Journal of Sedimentary Petrology, v. 47, p. 771–783.

Baas, J.H., 2004, Conditions for formation of massive turbiditic sandstones by primary depositional processes: Sedimentary Geology, v. 166, p. 293–310.

Bates, C., 1953, Rational theory of delta formation: American Association of Petroleum Geologists, Bulletin, v. 37, p. 2119–2162.

Bouma, A.H., 1962, Sedimentology of Some Flysch Deposits; A Basic Approach to Facies Interpretations: Amsterdam, Elsevier, 168 p.

Bouma, A.H., 2000, Coarse-grained and fine-grained turbidite systems as end member models: applicability and dangers: Marine and Petroleum Geology, v. 17, p. 137–143.

Britter, R.E., and Linden, P.F., 1980, The motion of the front of a gravity current travelling down an incline: Journal of Fluid Mechanics, v. 99, p. 531–543.

Cohen, A.S., and Thouin, C., 1987, Nearshore carbonate deposits in Lake Tanganyika: Geology, v. 15, p. 414–418.

de Rooij, F., and Dalziel, S.B., 2001, Time and space resolved measurements of deposition under turbidity currents, *in* McCaffrey, B., Kneller, B., and Peakall, J., eds., Particulate Gravity Currents: International Association of Sedimentologists, Special Publication 31, p. 207–215.

Dott, R.H, Jr, 1963, Dynamics of subaqueous gravity depositional processes: American Association of Petroleum Geologists, Bulletin, v. 47, p. 104–128.

Dutton, S.P., Flanders, W.A., and Barton, M.D., 2003, Reservoir characterization of a Permian deep-water sandstone, East Ford field, Delaware basin, Texas: American Association of Petroleum Geologists, Bulletin, v. 87, p. 609–627.

Forel, F.A., 1892, Le Léman: Monographie Limnologique, v. 1, Géographie, Hydrographie, Géologie, Climatologie, Hydrologie: Lausanne, Rouge, 543 p.

Gani, M.R., 2004, From turbid to lucid: Aô straightforward approach to sediment gravity flows and their deposits: SEPM, The Sedimentary Record, v. 23, p. 4–8.

Giovanoli, F., 1990, Horizontal transport and sedimentation by interflow and turbidity currents in Lake Geneva, *in* Tilzer, M.M., and Serruya, C., eds., Large Lakes: Ecological Structure and Function, p. 175–195.

Groeber, P., 1946, Observaciones geológicas a lo largo del meridiano 70°. Hoja Chos Malal: Asociación Geológica Argentina, Revista, v. 1–3, p. 177–208.

Groeber, P., 1953, Jurásico: Sociedad Argentina de Estudios Geográficos, v. 2, 347 p.

Gulisano, C.A., 1981, El ciclo Cuyano en el norte de Neuquén y sur de Mendoza: VIII Congreso Geológico Argentino, Buenos Aires, Argentina, Actas, v. 3, p. 579–592.

Gulisano, C.A., and Gutierrez Pleimling, A.R., 1995, The Jurassic of the Neuquén Basin. Neuquén Province: Buenos Aires, Secretaría de Minería de la Nación, Publicación no. 158, 111 p.

Herrero Ducloux, A., 1946, Contribución al conocimiento geológico del Neuquén extraandino: Boletín de Informacion Petrolera, v. 266, p. 245–280.

Hogg, S.L., 1993, Geology and Hydrocarbon potential of the Neuquén Basin: Journal of Petroleum Geology, v. 16, p. 383–396.

Hunter, R.E., 1977, Basic types of stratification in small aeolian dunes: Sedimentology, v. 24, p. 361–387.

Johnson, K.S., Paull, C.K., Barry, J.P., and Chavez, F.P., 2001, A decadal record of underflows from a coastal river into the deep sea: Geology, v. 29, p. 1019–1022.

Jopling, A.V., and Walker, R.G., 1968, Morphology and origin of ripple-drift cross lamination, with examples of Pleistocene of Massachusetts: Journal of Sedimentary Petrology, v. 38, p. 971–984.

Kempe, S., Kazmierczak, J., Landmann, G., Konuk, T., Reimer, A., and Lipp, A., 1991, Largest known microbialites discovered in Lake Van, Turkey: Nature, v. 349, p. 605–608.

Kersey, D.G., and Hsu, K.J., 1976, Energy relations and density current flows: an experimental investigation: Sedimentology, v. 23, p. 761–790.

Kineke, G.C., Woolfe, K.J., Kuehl, S.A., Milliman, J., Dellapenna, T.M., and Purdon, R.G., 2000, Sediment export from the Sepik River, Papua New Guinea: evidence forô aô divergent sediment plume: Continental Shelf Research, v. 20, p. 2239–2266.

Leclair, S.F., 2002, Preservation of cross-strata due to the migration of subaqueous dunes: an experimental investigation: Sedimentology, v. 49, p. 1157–1180.

Legarreta, L., 1985, Análisis estratigráfico de la Formación Huitrín (Cretácico Inferior), Provincia de Neuquén [Unpublished Ph.D. Thesis]: Universidad de Buenos Aires, 247 p.

Marteau, V., 2002, Los reservorios de la Formación Rayoso, *in* Schiuma, M., Hinterwimmer, G., and Vergani, G., eds., Rocas Reservorio de las Cuencas Productivas de la Argentina: Simposio del V Congreso de Exploración y Desarrollo de Hidrocarburos: Buenos Aires, Instituto Argentino del Petróleo y Gas, p. 511–528.

Mellere, M., Plink-Björklund, P., and Steel, R.J., 2002, Anatomy of shelf deltas at the edge of a prograding Eocene shelf margin, Spitsbergen: Sedimentology, v. 49, p. 1181–1206.

Métivier, F., Lajeunesse, E., and Cacas, M.C., 2005, Submarine canyons in the bathtub: Journal of Sedimentary Research, v. 75, p. 6–11.

Midtgaard, H.H., 1996, Inner-shelf to lower-shoreface hummocky sandstone bodies with evidence for geostrophic influenced combined flow, Lower Cretaceous, west Greenland: Journal of Sedimentary Research, v. 66, p. 343–353.

Mpodozis, C., and Ramos, V., 1989, The Andes of Chile and Argentina, *in* Ericksen, G.E., Cañas Pinochet, M.T., and Reinemud, J.A., eds., Geology of the Andes and Its Relation to Hydrocarbon and Mineral Resources: Circumpacific Council for Energy and Mineral Resources, Houston, Earth Sciences Series, v. 11, p. 59–90.

Mulder, T., and Alexander, J., 2001a, The physical character of subaqueous sedimentary density flows and their deposits: Sedimentology, v. 48, p. 269–299.

Mulder, T., and Alexander, J., 2001b, Abrupt change in slope causes variation in the deposit thickness of concentrated particle-driven density currents: Marine Geology, v. 175, p. 221–235.

Mulder, T., and Syvitski, J.P.M., 1995, Turbidity currents generated at river mouths during exceptional discharges to the world oceans: Journal of Geology, v. 103, p. 285–299.

Mulder, T., Syvitski, J.P.M., and Skene, K.I., 1998, Modeling of erosion and deposition of turbidity currents generated at river mouths: Journal of Sedimentary Research, v. 68, p. 124–137.

Mulder, T., Migeon, S., Savoye, B., and Jouanneau, J.M., 2001, Twentieth century floods recorded in the deep Mediterranean sediments: Geology, v. 29, p. 1011–1014.

Mulder, T., Syvitski, J.P.M., Migeon, S., Faugeres, J.C., and Savoye, B., 2003, Marine hyperpycnal flows: initiation, behaviour and related deposits. A review: Marine and Petroleum Geology, v. 20, p. 861–882.

Musacchio, E., and Vallati, P., 2000, La regresión del Barremiano–Aptiano en Bajada del Agrio, Neuquén (Argentina): Puerto Varas, IX Congreso Geológico Chileno, v. 2, p. 230–234.

Mutti, E., Gulisano, C.A., and Legarreta, L., 1994, Anomalous systems tracts stacking patterns within third order depositional sequences (Jurassic–Cretaceous Back Arc Neuquén Basin, Argentine Andes), *in* Posamentier, H.W., and Mutti, E., eds., Second High-Resolution Sequence Stratigraphy Conference, Tremp, Abstract Book, p. 137–143.

Mutti, E., Davoli, G., Tinterri, R., and Zavala, C., 1996, The importance of ancient fluvio-deltaic systems dominated by catastrophic flooding in tectonically active basins: Memorie di Scienze Geologiche, Universitá di Padova, v. 48, p. 233–291.

Mutti, E., Tinterri, R., Remacha, E., Mavilla, N., Angella, S., and Fava, L., 1999, An introduction to the analysis of ancient turbidite basins from an outcrop perspective: American Association of Petroleum Geologists, Continuing Education Course Note Series, v. 39, 96 p.

Mutti, E., Tinterri, R., Di Biase, D., Fava, L., Mavilla, N., Angella, S., and Calabrese, L., 2000, Delta-front faces associations of ancient flood-dominated fluvio-deltaic systems: Sociedad Geológica de España, Revista, v. 13, p. 165–190.

Mutti, E., Tinterri, R., Benevelli, G., Di Biase, D., and Cavanna, G., 2003, Deltaic, mixed and turbidite sedimentation of ancient foreland basins: Marine and Petroleum Geology, v. 20, p. 733–755.

Normark, W.R., and Piper, D.J.W., 1991, Initiation processes and flow evolution of turbidity currents: implications for the depositional record, *in* Osborne, R.H., ed., From Shoreline to Abyss: SEPM, Special Publication 46, p. 207–230.

Peakall, J., Felix, M., McCaffrey, B., and Kneller, B., 2001, Particulate gravity currents: Perspectives, *in* McCaffrey, B., Kneller, B., and Peakall, J., eds., Particulate Gravity Currents, International Association of Sedimentologists, Special Publication 31, p. 1–8.

Piper, D.J., Cochonat, P., and Morrison, M.L., 1999, The sequence of events around the epicentre of the 1929 Grand Banks earthquake: initiation of debris flows and turbidity current inferred from sidescan sonar: Sedimentology, v. 46, p. 79–97.

Plink-Björklund, P., and Steel, R.J., 2004, Initiation of turbidity currents: outcrop evidence for Eocene hyperpycnal flow turbidites: Sedimentary Geology, v. 165, p. 29–52.

Ponce, J.J., Zavala, C., Marteau, M., and Drittanti, D., 2002, Análisis estratigráfico y modelo deposicional para la Formación Rayoso (Cretácico Inferior) en la Cuenca Neuquina, Provincia del Neuquén, *in* Cabaleri, N., Cingolani, C.A., Linares, E., López de Luchi, M.G., Ostera, H.A., and Panarello, H.O., eds., XV Congreso Geológico Argentino, Actas, v. 1, p. 716–721.

Prior, D.B., Bornhold, B.D., Wiseman, W.J., and Lowe, D.R., 1987, Turbidity current activity in a British Columbia fjord Science, v. 237, p. 1330–1333.

Ramos, V.A., 1981, Descripción geológica de la hoja 33c, Los Chihuidos Norte, provincia del Neuquén: Argentina, Servicio Geológico Nacional, Boletín, v. 182, p. 1–103.

Remacha, E., Oms, O., and Coello, J., 1994, The Rapitán turbidite channel and its related eastern levee–overbank deposits, *in* Pickering, K., Ricci Lucchi, F., Smith, R., Hiscott, R., and Kenyon, N., eds., An Atlas of Deep-Water Systems: Turbidite System Architectural Style: London, Chapman & Hall, p. 21.1–21.4.

Sanders, J.E., 1965, Primary sedimentary structures formed by turbidity currents and related sedimentation mechanisms, *in* Middleton, G.V., ed., Primary Sedimentary Structures and Their Hydrodynamic Interpretation: Society of Economic Paleontologists and Mineralogists, Special Publication 12, p. 192–219.

Schumm, S.A., 1981, Evolution and response of the fluvial system; sedimentologic implications, *in* Ethridge, F.G., and Flores, R.M., eds., Recent and Ancient Nonmarine Depositional Environments: Society of Economic Paleontologists and Mineralogists, Special Publication 31, p. 19–29.

Shanmugam, G., 2000, 50 years of turbidite paradigm (1950s–1990s): deep-water processes and facies models—a critical perspective: Marine and Petroleum Geology, v. 17, p. 285–342.

Simons, D.B., Richardson, E.V., and Nordin, C.F., 1965, Sedimentary structures generated by flow on alluvial channels, *in* Middleton, G.V., ed., Primary Sedimentary Structures and Their Hydrodynamic Interpretation: Society of Economic Paleontologists and Mineralogists, Special Publication 12, p. 34–52.

Southard, J.B., 1991, Experimental determination of bedform stability: Annual Review of Earth and Planetary Sciences, v. 19, p. 423–455.

Storms, J.E.A., Van Dam, R.L., and Leclair, S., 1999, Preservation of cross-sets due to migration of current ripples over aggrading and non-aggrading beds: comparison of experimental data with theory: Sedimentology, v. 46, p. 189–200.

Stow, D.A.V., and Mayall, M., 2000, Deep-water sedimentary systems: new models for the 21st century: Marine and Petroleum Geology, v. 17, p. 125–135.

Twichell, D.C., Cross, V.A., Hanson, A.D., Buck, B.J., Zybala, J.G., and Rudin, M.J., 2005, Seismic architecture and lithofacies of turbidites in Lake Mead (Arizona and Nevada, U.S.A.), an analogue for topographically complex basins: Journal of Sedimentary Research, v. 75, p. 134–148.

Uliana, M., Dellape, D., and Pando, G., 1975a, Estratigrafía de las sedimentitas rayosianas (Cretácico Inferior de las provincias de Neuquén y Mendoza, Argentina): II Congreso Iberoamericano de Geología Económica, v. 1, p. 177–196.

Uliana, M., Delllape, D., and Pando, G., 1975b, Distribución y génesis de las sedimentitas rayosianas (Cretácico Inferior de las provincias de Neuquén y Mendoza, Argentina): II Congreso Iberoamericano de Geología Económica, v. 1, p. 151–176.

van den Berg, J.H., and van Gelder, A., 1993, A new bedform stability diagram, with emphasis on the transition of ripples to plane bed in flows over fine sands and silt, *in* Marzo, M., and Puigdefabregas, C., eds., Alluvial Sedimentation: International Association of Sedimentologists, Special Publication 17, p. 11–21.

Vergani, G.D., Tankard, A.J., Belotti, H.J., and Welsink, H.J., 1995, Tectonic evolution and paleogeography of the Neuquén basin, Argentina, *in* Tankard, A.J., Suárez, S.R., and Welsink, H.J., eds., Petroleum Basins of South America: American Association of Petroleum Geologists, Memoir 62, p. 383–402.

Zavala, C., and González, R., 2001, Estratigrafía del Grupo Cuyo (Jurásico inferior–medio) en la Sierra de la Vaca Muerta, Cuenca Neuquina: Boletín de Informaciones Petroleras, Tercera Época, año XVII, v. 65, p. 40–54.

Zavala, C., Ponce, J., and Marteau, M., 2001, Origin, sequence stratigraphy and hydrocarbon potential of the Rayoso Formation (Aptian–Albian) in the central Neuquén Basin (Argentina)(abstract):, American Association of Petroleum Geologists, Hedberg Conference ''New Technologies and New Play Concepts in Latin America,'' November 5–9, 2001, Mendoza, Argentina, Abstracts, p. 35–36.

Zollner, W., and Amos, A., 1973, Descripción geológica de la hoja 32-b, Chos Malal, Provincia de Neuquén: Argentina, Servicio Nacional de Minería y Geología, Boletín, 143 p.

Received 23 September 2004; accepted 18 April 2005.